

Research article

urn:lsid:zoobank.org:pub:10B6A707-DDA2-4D2F-9087-394933776459

Integrative taxonomy reveals two new cryptic species of *Hypseobrycon* Durbin, 1908 (Teleostei: Characidae) from the Maracaçumé and middle Tocantins River basins, Eastern Amazon region

Erick Cristofore GUIMARÃES^{1,*}, Pâmella Silva de BRITO²,
Pedro Henrique Negreiros BRAGANÇA³, Jadson Pinheiro SANTOS⁴, Axel Makay KATZ⁵,
Luis Fernando CARVALHO COSTA⁶ & Felipe Polivanov OTTONI⁷

^{1,2,4,7}Universidade Federal do Maranhão, Programa de Pós-Graduação em Biodiversidade e Biotecnologia da Amazônia Legal. Av. dos Portugueses 1966,
Cidade Universitária do Bacanga, CEP 65080-805, São Luís, MA, Brazil.

³South African Institute for Aquatic Biodiversity, Private Bag 1015,
Grahamstown, 6140, South Africa.

⁴Universidade Estadual do Maranhão, Laboratório de Ictiofauna e Piscicultura Integrada, Centro de Ciências Agrárias, Campus Paulo VI, avenida Lourenço Vieira da Silva, n. 1000, bairro Jardim São Cristóvão, CEP 65055-310, São Luís, MA, Brazil.

⁵Universidade Federal do Rio de Janeiro, Laboratório de Sistemática e Evolução de Peixes Teleósteos, Departamento de Zoologia, Instituto de Biologia, Cidade Universitária, CEP 21941-599. Rio de Janeiro, RJ, Brazil.

^{1,2,6}Universidade Federal do Maranhão, Departamento de Biologia, Laboratório de Genética e Biologia Molecular, Av. dos Portugueses 1966, Cidade Universitária do Bacanga, CEP 65080-805, São Luís, MA, Brazil.

^{1,2,7}Universidade Federal do Maranhão, Laboratório de Sistemática e Ecologia de Organismos Aquáticos, Centro de Ciências Agrárias e Ambientais, Centro de Ciências Agrárias e Ambientais (CCAA), campus de Chapadinha, BR-222, KM 04, S/N, Boa Vista, CEP 65500-000, Chapadinha, MA, Brazil.

*Corresponding author: erick.ictio@yahoo.com.br

²Email: pamellabrito@hotmail.com

³Email: pedrobra88@gmail.com

⁴Email: jadsonpesca@gmail.com

⁵Email: axelmk@gmail.com

⁶Email: lfecc@yahoo.com.br

⁷Email: fpottoni@gmail.com

¹urn:lsid:zoobank.org:author:67E9AADF-0B92-437E-BB31-6352FBC3F42D

²urn:lsid:zoobank.org:author:EBBAE3D2-5BB2-4D2A-8A0D-B2B7CC29DC4F

³urn:lsid:zoobank.org:author:59164A3E-8380-4672-A39C-C2FE563F3C4F

⁴urn:lsid:zoobank.org:author:7248FF02-D740-4E2D-A7E0-6A9E81F76974

⁵urn:lsid:zoobank.org:author:31E0031F-15ED-45B3-A0BB-CF985043D3B5

⁶urn:lsid:zoobank.org:author:2AE1615C-3F76-4867-9D7E-2942043F3D06

⁷urn:lsid:zoobank.org:author:6AB34592-DA6D-4AB7-88D8-1F63A97A12E3

Abstract. Two new species, *Hyphessobrycon frickei* Guimarães, Brito, Bragança, Katz & Ottoni sp. nov. and *H. geryi* Guimarães, Brito, Bragança, Katz & Ottoni sp. nov., are herein described, based on seven different and independent species delimitation methods, and on molecular and morphological characters, making the hypothesis of these new species supported from an integrative taxonomy perspective. They belong to the “Rosy tetra” clade, which is mainly characterized by the presence of a dark brown or black blotch on the dorsal fin and the absence of a midlateral stripe on the body. These two new species are distinguished from the other members of this clade mainly by the arrangement, shape and color pattern of humeral and dorsal-fin spots, as well as by other characters related to scale counts and body pigmentation. The placement of the new species within the “Rosy tetra” clade was based on the combination of morphological character states mentioned above and corroborated by a molecular phylogenetic analysis using the mitochondrial gene cytochrome oxidase subunit 1. In addition, a new clade (here termed *Hyphessobrycon copelandi* clade) within the “Rosy tetra” clade is proposed based on molecular data, comprising *H. copelandi*, *H. frickei* sp. nov., *H. geryi* sp. nov. and a still undescribed species. Our results corroborate the occurrence of hidden species within the “Rosy tetra” clade, as suggested by previous studies.

Keywords. ABGD, bPTP, DNA barcoding, GMYC, “Rosy tetra” clade.

Guimarães E.C., de Brito P.S., Bragança P.H.N., Brantos J.P., Katz A.M., Carvalho Costa L.F. & Ottoni F.P. 2020. Integrative taxonomy reveals two new cryptic species of *Hyphessobrycon* Durbin, 1908 (Teleostei: Characidae) from the Maracácumé and middle Tocantins River basins, Eastern Amazon region. *European Journal of Taxonomy* 723: 77–107. <https://doi.org/10.5852/ejt.2020.723.1145>

Introduction

Hyphessobrycon Durbin, 1908 is one of the most species-rich and widespread characid genus, comprising about 160 valid species and occurring from southern Mexico to the Río de La Plata in Argentina (Fricke *et al.* 2020a). Despite its non-monophyletic status (Mirande 2010; Oliveira *et al.* 2011; Betancur-R *et al.* 2018; Guimarães *et al.* 2018; Mirande 2018; Guimarães *et al.* 2019), *Hyphessobrycon* is one of the genera within Characidae whose species diversity has increased significantly in the past decades. Considering only the last decade, the number of species has risen from 109 to approximately 160, an increase of about 30% in the number of valid species (Fricke *et al.* 2020a), and currently comprising approximately 15% of all characid species (Fricke *et al.* 2020b).

In the absence of a stable phylogenetic definition, many species have been described and were assigned to *Hyphessobrycon* based on its traditional diagnosis by Eigenmann (1917, 1918). A similar practice has been commonly seen in other Characidae genera, such as *Hemigrammus* Gill, 1858 and *Knodus* Eigenmann, 1911 (Javonillo *et al.* 2010; Oliveira *et al.* 2011). Although the number of species of *Hyphessobrycon* has increased substantially, large knowledge gaps persist for the majority of species assigned to the genus, mainly regarding their phylogenetic position, e.g., *Hyphessobrycon brumado* Zanata & Camelier, 2010, *Hyphessobrycon frankei* Zarske & Géry, 1997, *Hyphessobrycon negodaguia* Lima & Gerhard, 2001 and *Hyphessobrycon wernerii* Géry & Uj, 1987.

In an attempt to deal with the high diversity within the genus, species groups were proposed (Géry 1977; Weitzman & Palmer 1997; García-Alzate *et al.* 2008; Carvalho & Malabarba 2015; Ota *et al.* 2020), such as: *Hyphessobrycon* groups a–f, “*callistus* group”, “Rosy tetra” clade, *Hyphessobrycon heterorhabdus* group, *Hyphessobrycon sensu stricto*, and *Hyphessobrycon panamensis* species group; some of them probably representing artificial operational assemblages to aid species identification, whereas others could represent potential monophyletic groups, with explicit putative synapomorphies (e.g., Castro-Paz *et al.* 2014; Bragança *et al.* 2015; Carvalho & Malabarba 2015; Guimarães *et al.* 2018, 2019).

Recent studies on Neotropical Characiformes, based on molecular data and species delimitation approaches, revealed a high cryptic diversity (e.g., Pereira *et al.* 2011; Melo *et al.* 2014; Benine *et al.* 2015; Benzaquem *et al.* 2015; Melo *et al.* 2016a, 2016b, 2016c; García-Melo *et al.* 2019). Similarly, three recently published papers (e.g., Castro-Paz *et al.* 2014; Guimarães *et al.* 2018, 2019) applied molecular species delimitation to investigate the species diversity within the “Rosy tetra” clade, and they all agreed that its taxonomy should be better investigated, since it includes cryptic species.

In addition to the wide distribution and the presence of cryptic species, the confuse taxonomic history of that clade is one of the main challenges when studying its diversity and relationships. The type species of *Hemigrammus*, *H. unilineatus* (Gill, 1858), and *Pristella* Eigenmann 1908, *P. maxillaris* (Ulrey, 1894), have been historically considered as closely related or belonging to the “Rosy-tetra” clade, which also includes the type species of *Hypessobrycon*, *H. compressus* (Meek, 1904) (Weitzman & Palmer 1997; Carvalho & Malabarba 2015). Thus, *Hypessobrycon* may be a putative synonym of *Hemigrammus* (Mirande 2010) or *Pristella*. However, further studies on the systematics of the species currently assigned to *Hypessobrycon* and close related genera are still necessary to clarify this issue (Guimarães *et al.* 2018, 2019).

The aim of this study is to describe two new cryptic species of *Hypessobrycon sensu* Bickford *et al.* (2006), members of the “Rosy tetra” clade, from the Maracáçumé and middle Tocantins River basins, Eastern Amazon region, based on an integrative taxonomy approach. Furthermore, a new subclade, within the “Rosy tetra” clade, is herein proposed.

Material and methods

Taxa sampling, specimen collection and preservation

Specimens were captured with manual trail-net (2 m long × 1.8 m high; mesh size: 2 mm) and euthanized in a buffered solution of ethyl-3-amino-benzoat-methanesulfonate (MS-222) with a concentration of 250 mg/l until completely ceasing opercular movements, according to animal welfare laws and guidelines (Close *et al.* 1996, 1997; Leary *et al.* 2013). Specimens selected for morphological analysis were fixed in formalin and left for ten days, after which they were preserved in 70% ethanol. Molecular data were obtained from specimens that were euthanized, fixed and preserved in absolute ethanol. Specimens used for morphological analysis are listed in type and comparative material lists. Specimens for molecular approaches are listed in Table 1. Sequences from other species of *Hypessobrycon* and allied species were obtained from the Barcode of Life Database (BOLD) and the National Center for Biotechnology Information (NCBI) databases (Table 1).

Morphological analysis

Measurements and counts were made according to Fink & Weitzman (1974). Vertical scale rows between the dorsal-fin origin and the lateral line do not include the scale of the median predorsal series situated just anterior to the first dorsal-fin ray. Counts of supraneurals, vertebrae, procurrent caudal-fin rays, unbranched dorsal- and anal-fin rays, branchiostegal rays, gill-rakers, premaxillary, maxillary, and dentary teeth, and other internal counts were taken only from cleared and stained (C&S) paratypes, prepared according to Taylor & Van Dyke (1985). The four modified vertebrae that constitute the Weberian apparatus were not included in the vertebrae counts, and the fused PU1 + U1 was considered as a single element. Osteological nomenclature follows Weitzman (1962). Institutional abbreviations follow Fricke & Eschmeyer (2020).

DNA extraction, amplification and sequencing analyses

DNA was extracted from fin clips using Wizard Genomic DNA Purification kit (Promega) according to the manufacturer’s protocol. Fragments of the mitochondrial cytochrome

Table 1 (continued on next two pages). Sampling sites, specimens and DNA sequence information included in the study. Sequences made available by this study are in bold.

Nº	Species	GenBank/BoldSystems	Catalog number
1	<i>Hyphessobrycon flammeus</i>	FUPR988-09	LBPV-40464
2	<i>Hyphessobrycon compressus</i>	FYPM054-10	CINV-NEC7411
3	<i>Hyphessobrycon compressus</i>	MXV767-15	ECO-CH P 7697
4	<i>Hyphessobrycon compressus</i>	MXV765-15	ECO-CH P 7697
5	<i>Hyphessobrycon compressus</i>	MXV766-15	ECO-CH P 7697
6	<i>Hyphessobrycon panamensis</i>	BSFFA760-07	STRI-05303
7	<i>Hyphessobrycon pyrrhonotus</i>	HYP040-13	INPA 37672-TRO10
8	<i>Hyphessobrycon pyrrhonotus</i>	HYP041-13	INPA 37672-TRO11
9	<i>Hyphessobrycon pyrrhonotus</i>	HYP157-13	JIR2003121101-6469
10	<i>Hyphessobrycon pyrrhonotus</i>	HYP158-13	JIR2003121101-6470
11	<i>Hyphessobrycon erythrostigma</i>	HYP076-13	INPA 37681-HERY1
12	<i>Hyphessobrycon erythrostigma</i>	HYP077-13	INPA 37681-HERY10
13	<i>Hyphessobrycon erythrostigma</i>	HYP078-13	INPA 37681-HERY2
14	<i>Hyphessobrycon erythrostigma</i>	HYP079-13	INPA 37681-HERY3
15	<i>Hyphessobrycon socolofi</i>	HYP131-13	INPA 39530-6152
16	<i>Hyphessobrycon socolofi</i>	HYP134-13	INPA 39530-6155
17	<i>Hyphessobrycon socolofi</i>	HYP148-13	INPA 39530-BCR8
18	<i>Hyphessobrycon socolofi</i>	HYP135-13	INPA 39530-6178 INPA 39530-6178
19	<i>Hyphessobrycon bentosi</i>	MK409672	–
20	<i>Hyphessobrycon bentosi</i>	MK240340	CICCAA02350
21	<i>Hyphessobrycon bentosi</i>	MK240341	CICCAA02351
22	<i>Hyphessobrycon bentosi</i>	MK240339	CICCAA02349
23	<i>Hyphessobrycon bentosi</i>	HYP117-13	INPA 39527-BA2
24	<i>Hyphessobrycon bentosi</i>	HYP116-13	INPA 39527-BA1
25	<i>Hyphessobrycon bentosi</i>	HYP097-13	INPA 37684-5939
26	<i>Hyphessobrycon bentosi</i>	HYP098-13	INPA 37684-5940
27	<i>Hyphessobrycon piorskii</i>	MG791915	CICCAA01659-1
28	<i>Hyphessobrycon piorskii</i>	MG791914	CICCAA01651-1
29	<i>Hyphessobrycon piorskii</i>	MF765796	CICCAA00725-1
30	<i>Hyphessobrycon piorskii</i>	MF765797	CICCAA00726-1
31	<i>Hyphessobrycon piorskii</i>	MK240337	CICCAA02164-1
32	<i>Hyphessobrycon piorskii</i>	MK240338	CICCAA0264-4
33	<i>Hyphessobrycon caru</i>	MH338230	CICCAA00748-1
34	<i>Hyphessobrycon caru</i>	MH338231	CICCAA00749-1
35	<i>Hyphessobrycon caru</i>	MH338232	CICCAA02300-1

Table 1 (continued).

Nº	Species	GenBank/BoldSystems	Catalog number
36	<i>Hypessobrycon caru</i>	MH338233	CICCAA02301-1
37	<i>Hypessobrycon micropterus</i>	BSB287-10	—
38	<i>Hypessobrycon micropterus</i>	BSB289-10	—
39	<i>Hypessobrycon micropterus</i>	BSB290-10	—
40	<i>Hypessobrycon micropterus</i>	BSB291-10	—
41	<i>Hypessobrycon simulatus</i>	GBOL1771-17	—
42	<i>Hypessobrycon simulatus</i>	GBOL3298-18	MHNG 2757.080
43	<i>Hypessobrycon simulatus</i>	GBOL3300-18	MHNG 2759.026
44	<i>Hypessobrycon simulatus</i>	GBOL3301-18	MHNG 2759.026
45	<i>Hypessobrycon simulatus</i>	GBOL3302-18	MHNG 2759.035
46	<i>Hypessobrycon eques</i>	DSMIS077-09	CBG OL 0544
47	<i>Hypessobrycon eques</i>	HYP070-13	INPA 37678-IC2
48	<i>Hypessobrycon eques</i>	HYP071-13	INPA 37679-PE1
49	<i>Hypessobrycon eques</i>	HYP072-13	INPA 37680-AL1
50	<i>Hypessobrycon geryi</i> sp. nov.	MK409673	CICCAA02047-1
51	<i>Hypessobrycon geryi</i> sp. nov.	MK409674	CICCAA02047-3
52	<i>Hypessobrycon geryi</i> sp. nov.	MK409675	CICCAA02047-6
53	<i>Hypessobrycon frickeyi</i> sp. nov.	MK409676	CICCAA02302-1
54	<i>Hypessobrycon frickeyi</i> sp. nov.	MK409677	CICCAA02302-2
55	<i>Hypessobrycon frickeyi</i> sp. nov.	MK409678	CICCAA02302-3
56	<i>Hypessobrycon copelandi</i>	HYP094-13	INPA 37683-TU1
57	<i>Hypessobrycon copelandi</i>	HYP095-13	INPA_37683-TU2
58	<i>Hypessobrycon copelandi</i>	HYP096-13	INPA_37683-TU3
59	<i>Hypessobrycon</i> aff. <i>copelandi</i>	HYP016-13	INPA_37666-MARA6
60	<i>Hypessobrycon</i> aff. <i>copelandi</i>	HYP017-13	INPA_37666-MARA7
61	<i>Hypessobrycon</i> aff. <i>copelandi</i>	HYP018-13	—
62	<i>Hypessobrycon</i> aff. <i>copelandi</i>	HYP019-13	—
63	<i>Hypessobrycon</i> <i>epicharis</i>	HYP002-13	INPA 37665-JUF1
64	<i>Hypessobrycon</i> <i>epicharis</i>	HYP004-13	INPA_37665-JUF3
65	<i>Hypessobrycon</i> <i>epicharis</i>	HYP005-13	INPA 37665-JUF4
66	<i>Hypessobrycon</i> <i>epicharis</i>	HYP006-13	INPA 37665-JUF8
67	<i>Hypessobrycon</i> cf. <i>sweglesi</i>	HYP026-13	INPA 37668-JAR3
68	<i>Hypessobrycon</i> cf. <i>sweglesi</i>	HYP027-13	INPA 37668-JAR4
69	<i>Hypessobrycon</i> cf. <i>sweglesi</i>	HYP028-13	INPA 37668-JAR5
70	<i>Hypessobrycon</i> cf. <i>sweglesi</i>	HYP030-13	INPA 37668-JAR7
71	<i>Hypessobrycon</i> <i>roseus</i>	GBOL759-15	—

Table 1 (continued).

Nº	Species	GenBank/BoldSystems	Catalog number
72	<i>Hyphessobrycon roseus</i>	GBOL1785-17	–
73	<i>Hyphessobrycon roseus</i>	GBOL760-15	–
74	<i>Hyphessobrycon roseus</i>	GBOL3336-18	–
75	<i>Pristella maxillaris</i>	KU568982.1	–
76	<i>Pristella maxillaris</i>	KU568981.1	–
77	<i>Pristella maxillaris</i>	TZGAA025-06	I012-1.3
78	<i>Pristella maxillaris</i>	TZGAA178-06	I014-7.4
79	<i>Moenkhausia hemigrammoides</i>	HYP101-13	INPA 38532-PR1
80	<i>Moenkhausia hemigrammoides</i>	HYP102-13	INPA 38532-PR2
81	<i>Moenkhausia hemigrammoides</i>	HYP103-13	INPA 38532-PR3

c oxidase subunit 1 gene were amplified, using the universal primers designed by Ward *et al.* (2005) (FISHF1 5'-TCAACCAACCACAAAGACATTGGCAC-3' and FISHR1 5'-TAGACTCTGGGTGGCCAAAGAATCA-3'). Polymerase chain reactions (PCR) comprised a total volume of 15 µl containing 1× Polymerase buffer, 1.5 mM MgCl₂, 200 µM dNTP, 0.2 uM of each primer, 1U of Taq Polymerase (Invitrogen), 100 ng of DNA template, and ultrapure water. The PCR cycles were as follows: 2 min at 94°C, followed by 35 cycles of 94°C for 30s, 54°C for 30s, and 72°C for 1 min, and 10 min at 72°C. Amplicons were purified using Illustra GFX PCR DNA and Gel Purification Kit (GE Healthcare Systems) and sequenced using the forward primer by an outsourced sequencing service at the University of São Paulo, using BigDye Terminator kit ver. 3.1 Cycle Sequencing kit in ABI 3730 DNA Analyser (Applied Biosystems).

Data partition, evolution models, and alignment

The dataset cytochrome c oxidase subunit 1 (COI) (639 bp). Sequences were aligned using ClustalW (Chenna *et al.* 2003). The DNA sequences were translated into amino acids residues to test for the presence of premature stop codons or indels using the program MEGA 7 (Kumar *et al.* 2016). Measure Substitution Saturation tests were performed in DAMBE5 (Xia 2013) according to the algorithm proposed by Xia *et al.* (2003). The best-fit evolutionary model (GTR+G) was calculated, using the corrected Akaike Information Criterion (AICc) determined by the jModelTest 2.1.7 (Darriba *et al.* 2012).

Species concept, species delimitation, and diagnoses

The unified species concept is herein adopted by expressing the conceptual definition shared by all traditional species concepts – “species are (segments of) separately evolving metapopulation lineages” – disentangling operational criterion elements to delimit taxa from species concepts (de Queiroz 2005, 2007). According to this concept, species are treated as hypothetical units and could be tested (detected) by the application of distinct criteria (species delimitation methods) (de Queiroz 2005, 2007). It allows for any method to independently provide evidence about species limits and identities (de Queiroz 2005, 2007).

Seven distinct and independent methods relying on different operational criteria for sp suzu65@gmail.com species delimitation, based on morphological and molecular data, were implemented here: PAA, Population Aggregation Analysis (Davis & Nixon 1992); DBC, DNA barcoding, as proposed by Hebert *et al.* (2003a, 2003b, 2004a, 2004b); ABGD, Automatic Barcode Gap Discovery (Puillandre *et al.* 2012);

WP, a tree-based method as proposed by Wiens & Penkrot (2002) (following Sites & Marshall 2003); CBB, a character-based DNA barcoding as proposed by Desalle *et al.* (2005); as well as two coalescent species delimitation methods termed bPTP, the Bayesian implementation of the Poisson tree processes (Zhang *et al.* 2013), and GMYC, the General Mixed Yule Coalescent method , single-threshold version (Fujisawa & Barraclough 2013).

All species delimitation methods here adopted, except PAA that relies only on morphological characters, were performed using cytochrome c oxidase subunit 1 (COI) sequences, since it is a mitochondrial gene with a fast evolutionary rate, thus suitable and widely used for single locus species delimitation approaches (Avise 2000).

Population aggregation analysis (PAA)

The PAA (Davis & Nixon 1992) is a character-based method, in which species are delimited by a unique combination of morphological character states occurring in one or more populations (Costa *et al.* 2014). Basically, the occurrence of the same character state in individuals from different populations is evidence to the presence of a gene flow between them, indicating that all correspond to the same species (lineage), whereas the presence of exclusive character states not shared between individuals belonging to two distinct populations suggests that there is no gene flow between them, thus corresponding to distinct lineages.

Wiens and Penkrot analysis (WP)

WP is based on the direct inspection of haplotype trees generated by a phylogenetic analysis having as terminals at least two individuals (haplotypes) of each focal species. In this method, the term ‘exclusive’ is used instead of monophyletic, since the term monophly is considered inapplicable below the species level (Wiens & Penkrot 2002). Clustered haplotypes with a concordant geographic distribution forming mutual and well supported clades (exclusive lineages) are considered as strong evidence for species discrimination (absence of gene flow with other lineages). When haplotypes from the same locality fail to cluster together, there is potential evidence for gene flow with other populations (Wiens & Penkrot 2002). Haplotype tree statistical support was assessed by the posterior probability value, considered as significant at about 0.95 or higher (Alfaro & Holder 2006). When only one haplotype (specimen) from one putative population was available, the species delimitation was based on the exclusivity of the sister clade of this single haplotype, supported by significant values, allowing us to perform the test in populations with only one haplotype (Wiens & Penkrot 2002). In addition, the method allows the recognition of nonexclusive lineages as species since their sister clades are exclusive and supported by significant values (Wiens & Penkrot 2002).

A Bayesian inference-based phylogenetic (BI) tree was estimated in MrBayes (Huelsenbeck & Ronquist 2001) plugin in Geneious 9.0.5 to reconstruct the evolutionary relationships among terminals using General Time Reversible (GTR+G) as evolutionary model. The Bayesian tree inference was based on a chain length of 10 million, a burn-in length of 500 000 generations subsampling trees every 10 000 generations. We used a sequence of *Hyphessobrycon flammatus* Myers, 1924 as outgroup, and all the other haplotypes were considered as ingroup in our analysis..

Traditional DNA barcoding (DBC)

We used the Kimura-2-parameters model (K2P) (Kimura 1980) to estimate the pairwise genetic distances between species in MEGA 7 software (Kumar *et al.* 2016). We used DnaSP ver. 6. (Rozas *et al.* 2003) to estimate the number of variable sites and haplotypes. We considered a cutoff of 2% as sufficient to discriminate species, since this threshold is commonly inferred by species delimitations among Neotropical fish species based on COI (Jacobina *et al.* 2018).

Character-based DNA barcoding (CBB)

The CBB is similar to the population aggregation analysis proposed by Davis & Nixon (1992), but directed to nucleotides as an alternative method for diagnosing taxa through DNA barcodes (De Salle *et al.* 2005), since the original method is based on subjective cut-off distance thresholds for the inference of species limits (Hebert *et al.* 2003a, 2003b, 2004a, 2004b). This method delimits species by the presence of a unique combination of nucleotides within a site shared by individuals of the same population or group of populations. In addition, species were diagnosed by nucleotide substitutions (Costa *et al.* 2014; Ottoni *et al.* 2019). Nucleotide substitutions among lineages were optimized in the Bayesian inference topology using PAUP ver. 4 (Swofford 2002). Each nucleotide substitution is represented by its relative numeric position determined through sequence alignment with the complete mitochondrial genome of *Astyanax paranae* Eigenmann, 1914 (KX609386.1:5503-7062), followed by the specific nucleotide substitution in parentheses. The results of this analysis are presented in Appendix 2 and the molecular diagnosis sections.

General Mixed Yule Coalescent (GMYC)

The GMYC is a single locus coalescent phylogeny-based species delimitation approach that relies on the branch length to establish a threshold between speciation and coalescent processes (Fujisawa & Barraclough 2013). Here we applied the single-threshold version of the method, which usually outperforms the multiple-threshold version (Fujisawa & Barraclough 2013). Following to the requirements of this method,, the dataset was reduced to include only unique haplotypes of *H. piorskii*, *H. caru*, *H. geryi* sp. nov., *H. copelandi* Durbin, 1908, *H. frickei* sp. nov.; *H. aff. copelandi*, and the outgroup was restricted to *Hyphessobrycon bentosi* Durbin, 1908. Sequences were aligned using ClustalW (Chenna *et al.* 2003). The best-fit evolutionary model (GTR+G) for the reduced dataset was calculated using the corrected Akaike Information Criterion (AICc) determined by the jModelTest ver. 2.1.7 (Darriba *et al.* 2012). The input ultrametric phylogenetic tree was performed in BEAST ver. 1.8.4 (Drummond *et al.* 2012), with the following parameters: an uncorrelated relaxed clock with lognormal distribution, a Yule Process as tree prior with 10 million generations and sampling frequency of 1000. The GMYC analysis was performed in the Exelixis Lab's server <https://species.h-its.org/gmyc/>.

Bayesian implementation of the poisson tree processes (bPTP)

The bPTP is another single locus coalescent phylogeny-based species delimitation method, but it differs from other unilocus species delimitation coalescent approaches, such as GMYC, because it does not need an ultrametric tree (not relying on branch length to delimit species), thus avoiding errors and computer intensive processes (Zhang *et al.* 2013). The method assumes that more molecular variability (number of nucleotide substitutions) is expected between haplotypes from different species than within a species (Zhang *et al.* 2013), establishing a threshold between speciation and coalescent processes. The reduced dataset and the input phylogenetic tree for performing the bPTP was the same used in GMYC species delimitation method ,since this method also requires the use of only unique haplotypes, and previously detailed in the GMYC species delimitation method description. The bPTP analysis was performed in the Exelixis Lab's web server <http://species.h-its.org/ptp/>, following the default parameters except for a 20% burn-in.

Automatic Barcode Gap Discovery (ABGD)

The ABGD is a barcode species delimitation method that aims to establish a minimum gap that probably corresponds to the threshold between interspecific and intraspecific processes (Puillandre *et al.* 2012). The major advantage of ABGD when compared to the other barcode species delimitation methods is that the inference of the limit between interspecific and intraspecific processes (gap detection) is recursively applied to previously obtained groups to get finer partitions until there is no

further partitioning, allowing a more refined search. Basically, the ABGD analysis indicates the number of groups (species) estimated relative to a large spectrum of p values (prior intraspecific values) in which a 0.1 value assumes a maximum intraspecific variability indicating that all sequences belong to only one species, whereas a 0.001 value assumes a very small intraspecific variability indicating that each distinct haplotype represents a different species. After running the ABGD, additional molecular, morphological or ecological characters are needed to infer the correct number of species, following an integrative taxonomy perspective. The ABGD analysis was performed on the ABGD server website <https://bioinfo.mnhn.fr/abi/public/abgd/abgdweb.html> following the default parameters.

Results

Description of new species

Order Characiformes Regan, 1911
 Family Characidae Latreille, 1825
 Genus *Hypessobrycon* Durbin, 1908

Hypessobrycon frickei Guimarães, Brito, Bragança, Katz & Ottoni sp. nov.

urn:lsid:zoobank.org:act:6FECEAF1-EBFC-4978-9861-E502AB12A5C5

Fig. 1, Table 2

Morphological Diagnosis (PAA)

Hypessobrycon frickei Guimarães, Brito, Bragança, Katz & Ottoni sp. nov. clearly differs from most of its congeners, except members of the “Rosy tetra” clade, by the presence of a dark brown or black blotch on the dorsal fin (vs absence) and the absence of a midlateral stripe on the body (vs presence). The new species differs from most of its congeners within the “Rosy tetra” clade by possessing a conspicuous small, slightly vertical and elliptical humeral spot (Fig. 1) (vs inconspicuous vertically elongated) humeral spot in *Hypessobrycon bentosi* Durbin, 1908, *H. caru* Guimarães, De Brito, Feitosa, Carvalho-Costa, Ottoni, 2018, *H. hasemani* Fowler, 1913, *H. piorskii* Guimarães, De Brito, Feitosa, Carvalho-Costa, Ottoni, 2018; an approximately rounded humeral spot in *H. erythrostigma* (Fowler, 1943), *H. jackrobertsi* Zarske, 2014, *H. minor* Durbin, 1909, *H. pando* Hein, 2009, *H. paepkei* Zarske, 2014, *H. pyrrhonotus* Burgess, 1993, *H. roseus* (Géry, 1960), *H. socolofi* Weitzman, 1977, and *H. sweglesi* (Géry, 1961); a conspicuous horizontal or posteriorly elongated humeral spot in *H. epicharis* Weitzman & Palmer, 1997, *H. khardinae* Zarske, 2008, and *H. werneri* Géry & Uj, 1987; a large vertical conspicuous humeral spot at least on males in *H. eques* (Steindachner, 1882), *H. haraldschultzi* Travassos, 1960, *H. micropterus* (Eigenmann, 1915), *H. megalopterus* (Eigenmann, 1915), *H. simulatus* (Géry, 1960) and *H. takasei* Géry, 1964; and the absence of a humeral spot in *H. compressus* (Meek, 1904), *H. dorsalis* Zarske, 2014, *H. georgettae* Géry, 1961, *H. pulchripinnis* Ahl, 1937, and *H. rosaceus* Durbin, 1909 (see Guimarães et al. 2019: fig. 2). The new species furthermore differs from *H. copelandi* Durbin, 1908 and *H. haraldschultzi* Travassos, 1960 by the number of scales on the lateral series (33–37 vs 29–31, 28–30 lateral line scales, respectively); and from *H. geryi* Guimarães, Brito, Bragança, Katz & Ottoni sp. nov. by the number of horizontal scale rows between the lateral line and pelvic-fin origin (3 vs 4–5, modally 4). Furthermore, *H. frickei* sp. nov differs from *H. geryi* sp. nov. by the absence of conspicuous dark chromatophores on opercular zone (vs presence); the absence of conspicuous dark chromatophores on the region posterior to the humeral spot (vs presence, extending to the end of the caudal peduncle); the absence of a thin vertical line, formed by a concentration of dark chromatophores at the middle of the humeral spot, extending to one to two scales above and below the spot (vs presence); and dorsal-fin base less pigmented (vs conspicuous pigmentation on dorsal-fin base) (see Figs 1, 4–5).

Molecular diagnosis (CBB)

Hyp Hessobrycon frickei Guimarães, Brito, Bragança, Katz & Ottoni sp. nov. is a member of the *H. copelandi* clade, possessing the following 25 nucleotide substitutions: COI 90 (C→A), COI 126 (A→G), COI 138 (C→T), COI 189 (C→T), COI 192 (T→A), COI 237 (C→T), COI 264 (T→C), COI 282 (C→T), COI 285 (C→A), COI 312 (T→C), COI 384 (C→T), COI 402 (A→G), COI 429 (A→G), COI 435 (A→G), COI 486 (T→C), COI 522 (A→G), COI 525 (C→T), COI 547 (C→T), COI 582 (T→C), COI 621 (T→C), COI 624 (A→G), COI 678 (T→C), COI 684 (A→C), COI 690 (T→C), COI 696 (A→G). In addition, it differs from *H. geryi* sp. nov. by possessing the following nine nucleotide substitutions: COI 231 (T→C), COI 315 (A→G), COI 345 (A→C), COI 375 (G→A), COI 402 (G→A), COI 405 (T→C), COI 528 (A→G), COI 558 (A→G), COI 609 (A→G); and from *A. copelandi* by possessing the following eleven nucleotide substitutions: COI 126 (G→A), COI 141 (G→C), COI 291 (A→G), COI 300 (A→G), COI 345 (C→G), COI 366 (C→T), COI 435 (G→A), COI 510 (T→C), COI 633 (T→C), COI 657 (C→T), COI 672 (T→C).

Etymology

The new species is named after the ichthyologist Ronald Fricke, in recognition of his contribution to ichthyology.

Material examined

Holotype

BRAZIL • 18.8 mm SL; Maranhão State, Maracaçumé municipality, Maracaçumé River; 2°3'14" S, 45°57'16" W; 29 Jan. 2017; E.C. Guimarães and P.S. Brito leg; CICCAA 02363

Paratypes

BRAZIL • 10 specs; 14.8–19.6 mm SL; Maranhão State, Maracaçumé municipality; stream tributary to the Maracaçumé River basin; 2°08'38" S, 45°47'22" W; 29 Jan. 2017; Guimarães E.C., Brito P.S. leg.; CICCAA 02362 • 5 specs; 15.5–17.7 mm SL (C&S); same collection data as for preceding; collected with holotype; CICCAA 02388 • 1 spec.; 17.8 mm SL; same collection data as for preceding; UFRJ 6918.

Type locality

Maracaçumé River basin, a coastal river in the Maranhão state, northeastern Brazil (Fig. 3).

Description

Morphometric data of holotype and paratypes are presented in Table 2.

BODY. Small (larger specimen with 19.6 mm of SL), laterally compressed, moderately deep, greatest body depth slightly anterior to dorsal-fin base; body profile straight and downward directed from the end of dorsal fin to adipose fin, straight or slightly convex between latter point and origin of dorsal most procurrent caudal-fin ray; dorsal profile of head convex from upper lip to vertical through eye; predorsal profile of body roughly straight, dorsal-fin base slightly convex, posteroventrally inclined; ventral profile of head convex from lower jaw to pelvic-fin origin; straight and posterodorsally slanted along anal-fin base; and slightly concave on caudal peduncle. Jaws equal, mouth terminal. Maxilla reaching vertical to anterior margin of pupil.

TEETH. Premaxillary teeth in two rows. Outer row with two tricuspid teeth; inner row with 3(10), pentacuspid teeth and 3(7) or 2(3) tricuspid teeth. Maxilla with 2(5) or 3(6) tricuspid teeth. Dentary with five (10) larger pentacuspid teeth followed by five (8) or six (2) smaller tricuspid teeth tooth (Fig. 2).



Fig. 1. *Hyphessobrycon frickei* Guimarães, Brito, Bragança, Katz & Ottoni sp. nov., holotype (CICCAA 02363), 18.8 mm SL; Brazil: Maranhão State: Maracaçumé River basin.

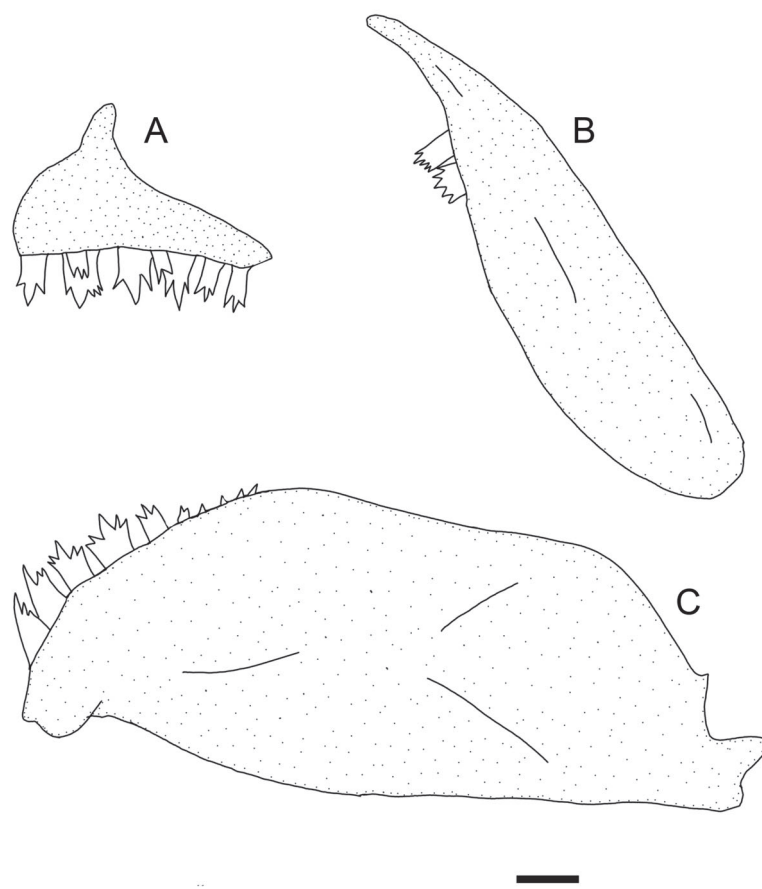


Fig. 2. *Hyphessobrycon frickei* Guimarães, Brito, Bragança, Katz & Ottoni sp. nov. (CICCAA 02388), 17.7 mm SL; jaw suspensory. **A.** Premaxillary. **B.** Maxilla. **C.** Dentary. Scale bar: 1 mm

Table 2. Morphometric data ($N = 18$) for the holotype and paratypes of *Hyphessobrycon frickei* Guimarães, Brito, Bragança, Katz & Ottoni sp. nov., SD = Standard deviation.

	Holotype	Paratypes	Mean	SD
Standard length	18.8	14.8–19.6	17.4	–
Percentages of standard length				
Depth at dorsal-fin origin (body depth)	30.8	28.4–32.8	30.5	1.2
Snout to dorsal-fin origin	50.7	47.2–52.1	50.0	1.2
Snout to pectoral-fin origin	28.6	26.2–30.7	28.2	1.4
Snout to pelvic-fin origin	44.6	43.1–47.5	45.1	1.3
Snout to anal-fin origin	58.5	57.0–62.2	59.3	1.4
Caudal peduncle depth	9.7	8.6–11.0	10.0	0.7
Caudal peduncle length	11.4	9.1–12.1	10.4	0.9
Pectoral-fin length	20.4	17.5–22.7	19.6	1.3
Pelvic-fin length	17.1	16.0–19.3	17.3	0.9
Dorsal-fin base length	14.7	13.5–16.3	14.8	1.0
Dorsal-fin height	27.4	27.2–33.1	29.1	1.6
Anal-fin base length	33.2	30.8–35.3	33.1	1.0
Eye to dorsal-fin origin	35.6	32.5–37.3	34.4	1.1
Dorsal-fin origin to caudal-fin base	56.5	51.1–56.3	53.4	1.4
Head length	28.2	26.7–30.9	28.7	1.2
Percentages of head length				
Horizontal eye diameter	41.8	40.6–45.9	42.7	1.6
Snout length	22.8	17.5–24.0	21.6	1.9
Least interorbital width	25.7	24.1–30.6	27.4	1.7
Upper jaw length	36.5	33.2–37.6	35.3	1.6

SCALES. Scales cycloid, three to eight radii strongly marked, circuli well-marked anteriorly, weakly marked posteriorly; lateral line incompletely pored, with 7(6), 8(7)*, 9(3) or 10(1) perforated scales. Longitudinal scales series including lateral-line (perforated) scales 33(1), 34(1), 35(3), 36(7)* or 37(1). Longitudinal scales rows between dorsal-fin origin and lateral line 5(1) or 6(16)*. Horizontal scale rows between lateral line and pelvic-fin origin 3(17)*. Scales in median series between tip of supraoccipital spine and dorsal-fin origin 8(3) or 9(14). Circumpeduncular scales 10(12)*, 11(3) or 12(2).

FINS. Dorsal-fin origin at midbody. Base of last dorsal-fin ray at vertical through first third of anal-fin. Dorsal-fin rays ii + 9(10)*, iii + 9(5), ii + 10(2). First dorsal fin pterygiophore main body located behind neural spine of 4th vertebrae. Adipose fin present. Anal-fin origin aligned with vertical line through middle of dorsal-fin, between 6th and 8th dorsal-fin rays. Anteriormost anal-fin pterygiophore inserting posterior to haemal spine of 11th vertebrae. Anal-fin origin aligned with vertical line through middle of dorsal fin (between base of 6th and 8th dorsal-fin rays). Anal fin iii + 22(10)* or iii + 23(7); anterior anal-fin margin slightly convex, with anteriormost rays more elongate and slightly more thickened than remaining rays, forming a distinct lobe. Remaining rays smaller with straight distal margin. Pectoral-fin rays 12(17)*. Tip of pectoral fin surpassing pelvic-fin base. Pelvic-fin rays 8(17)*, surpassing anal-fin

origin. Caudal fin forked, upper and lower lobes similar in size. Principal caudal fin rays 11+10(10)* or 10+9(7); dorsal procurrent rays 8(2) or 9(3) and ventral procurrent rays 7(2) or 8(3).

OSTEOLOGICAL COUNTS. Branchiostegal rays 4(5). First gill arch with 1(4), 2(1) hypobranchial, 11(1), 12(3), or 13(1) ceratobranchial, 1(5) cartilage between ceratobranchial and epibranchial, and 5(1) or 6(4) epibranchial gill-rakers. Supraneurals 4(4) or 5(1). Precaudal vertebrae 11 (5) and caudal vertebrae 19 (5). Total vertebrae 30(5).

Coloration in alcohol (Fig. 1)

Ground coloration light yellowish brown. Humeral spot conspicuous, slightly vertically elliptical. Flank with inconspicuous chromatophores, more concentrated on dorsal and ventral regions; middle region without or with inconspicuous chromatophores. Ventral region lacking dark brown chromatophores. Dark brown chromatophores present on dorsal portion of head and tip of snout, becoming sparser or absent on opercular region, and absent on cheek. Dorsal-fin ground coloration hyaline, with conspicuous black or dark brown spot located on anterior portion of fin, reaching about 6th ray, approximately between half to two thirds of fin depth. Dorsal-fin base with inconspicuous scattered chromatophores. Anal and caudal fins hyaline. Anal and caudal fins with a darker, usually dark brown, posterior margin. Adipose fin hyaline to light brown, with dark chromatophores at margin and posterior portion. Pectoral and pelvic fins hyaline; pelvic fin with variable amounts of dark brown pigmentation remaining depending on specimen preservation state.

Sexual dimorphism

Bony hooks on fins are absent in all examined specimens. According to Malabarba & Weitzman (2003), the presence of bony hooks is a common dimorphic feature among characid species. Although this sexual dimorphism is not observed in all characid species, as in the case of the species described here.

Color pattern is not sexually dimorphic either.

Hypseobrycon geryi Guimarães, Brito, Bragança, Katz & Ottoni sp. nov.

urn:lsid:zoobank.org:act:75667753-6AB4-4E18-BBD6-3C33ECE68CD4

Figs 4–6, Table 3

Morphological diagnosis (PAA)

Hypseobrycon geryi Guimarães, Brito, Bragança, Katz & Ottoni sp. nov. clearly differs from most of its congeners, except members of the “Rosy tetra” clade, by the presence of a dark brown or black blotch on the dorsal fin (vs absence) and the absence of a midlateral stripe on the body (vs presence). The new species differs from most of its congeners from the “Rosy tetra” clade by possessing a conspicuous small slightly vertical elliptical humeral spot (Fig. 1) (vs inconspicuous vertically elongated) humeral spot in *Hypseobrycon bentosi* Durbin, 1908, *H. caru* Guimarães, De Brito, Feitosa, Carvalho-Costa, Ottoni, 2018, *H. hasemani* Fowler, 1913, *H. piorskii* Guimarães, De Brito, Feitosa, Carvalho-Costa, Ottoni, 2018; approximately rounded humeral spot in *H. erythrostigma* (Fowler, 1943), *H. jackrobertsi* Zarske, 2014, *H. minor* Durbin, 1909, *H. pando* Hein, 2009, *H. paepkei* Zarske, 2014, *H. pyrrhonotus* Burgess, 1993, *H. roseus* (Géry, 1960), *H. socolofi* Weitzman, 1977, and *H. sweglesi* (Géry, 1961); humeral spot horizontally or posteriorly elongated in *H. epicharis* Weitzman & Palmer, 1997, *H. khardinae* Zarske, 2008, and *H. werneri* Géry & Uj, 1987; large vertical conspicuous humeral spot at least on males in *H. eques* (Steindachner, 1882), *H. haraldschultzi* Travassos, 1960, *H. micropterus* (Eigenmann, 1915), *H. megalopterus* (Eigenmann, 1915), *H. simulatus* (Géry, 1960) and *H. takasei* Géry, 1964; and absence of humeral spot in *H. compressus* (Meek, 1904), *H. dorsalis* Zarske, 2014, *H. georgettae* Géry, 1961, *H. pulchripinnis* Ahl, 1937, and *H. rosaceus* Durbin, 1909 (Guimarães et al. 2019: fig. 2). The new species herein described differs from *H. copelandi* Durbin, 1908, *H. haraldschultzi* Travassos,

1960 by the number of lateral series of scales (34–37 vs 29–31, 28–30 lateral line scales, respectively); from *H. frickei* Guimarães, Brito, Bragança, Katz & Ottoni sp. nov. by the number of horizontal scale rows between lateral line and pelvic-fin origin (4–5, modally 4 vs 3); presence of conspicuous dark chromatophores on opercular zone (vs absence); presence of conspicuous dark chromatophores on the region posterior to humeral spot, extending to the end of caudal peduncle (vs absence); presence of a thin vertical line, formed by the concentration of dark chromatophores, at middle of humeral spot, extending one to two scales above and below the spot (vs absence); and dorsal-fin base with conspicuous pigmentation (vs less pigmented) (see Figs 1, 4–5).

Molecular diagnosis (CBB)

Hyphessobrycon geryi Guimarães, Brito, Bragança, Katz & Ottoni sp. nov. is a member of the *H. copelandi* clade, possessing the following 25 nucleotide substitutions: COI 90 (C→A), COI 126 (A→G), COI 138 (C→T), COI 189 (C→T), COI 192 (T→A), COI 237 (C→T), COI 264 (T→C), COI 282 (C→T), COI 285 (C→A), COI 312 (T→C), COI 384 (C→T), COI 402 (A→G), COI 429 (A→G), COI 435 (A→G), COI 486 (T→C), COI 522 (A→G), COI 525 (C→T), COI 547 (C→T), COI 582 (T→C), COI 621 (T→C), COI 624 (A→G), COI 678 (T→C), COI 684 (A→C), COI 690 (T→C), COI 696 (A→G). In addition, it differs from the other species of this group by the following eight nucleotide substitutions: COI 225 (T→C), COI 228 (A→C), COI 321 (G→A), COI 522 (G→A), COI 534 (G→A), COI 543 (A→G), COI 589 (C→T), COI 615 (G→A).

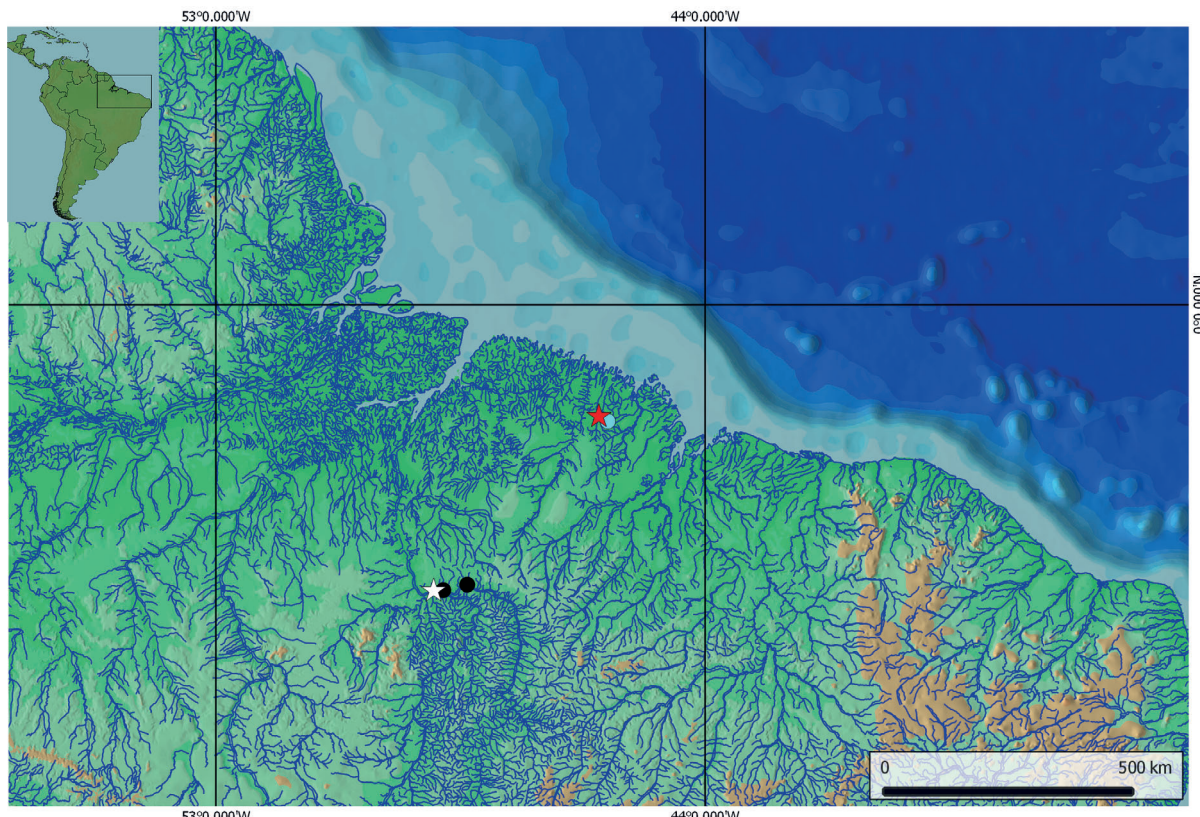


Fig. 3. Geographical distribution of *Hyphessobrycon frickei* Guimarães, Brito, Bragança, Katz & Ottoni sp. nov. and *H. geryi* Guimarães, Brito, Bragança, Katz & Ottoni sp. nov. Red star denotes holotype and blue circle denotes paratypes of *H. frickei* Guimarães, Brito, Bragança, Katz & Ottoni sp. nov. whereas white star denotes holotype and the black circles denote paratypes of *H. geryi* Guimarães, Brito, Bragança, Katz & Ottoni sp. nov.

Etymology

The new species is named after the ichthyologist Jacques Géry (in memoriam) in recognition of his scientific contribution on Characiformes.



Fig. 4. *Hyphessobrycon geryi* Guimarães, Brito, Bragança, Katz & Ottoni sp. nov., holotype (CICCAA 02403), 28.3 mm SL; Brazil: Maranhão State: Lower Tocantins River basin.



Fig. 5. *Hyphessobrycon geryi* Guimarães, Brito, Bragança, Katz & Ottoni sp. nov., paratype (CICCAA 02348), 22.7 mm SL; Brazil: Maranhão State: Lower Tocantins River basin; living specimen photographed immediately after collection.

Material examined

Holotype

BRAZIL • 27.8 mm SL; Pará State, Marabá municipality, Flexeiras River, Tocantins River basin; 5°15'38" S, 48°59'35" W; 20 Sep. 2016; E.C. Guimarães and C.H. Costa; CICCAA 02403

Paratypes

BRAZIL – **Pará State** • 1 spec.; 25.6 mm SL; same collection data as for holotype; CICCAA 00722 • 13 specs; 15.9–19.5 mm SL; Marabá municipality, Flexeiras River, Tocantins River basin; 5°15'38" S, 48°59'35" W; 21 Sep. 2018; E.C. Guimarães and P.S. Brito leg.; CICCAA 02358 • 11 specs; 16.9–19.2 mm SL; Marabá municipality, Flexeiras River, Tocantins River basin; 5°15'38" S, 48°59'35" W; 9 Mar. 2018; E.C. Guimarães and P.S. Brito leg.; CICCAA 02359 • 11 specs; 18.8–22.2 mm SL; Bom Jesus do Tocantis, Jacundá River, Tocantins River basin; 5°15'1"S, 48°48'58" W; 21 Dec. 2017; E.C. Guimarães and P.S. Brito leg.; CICCAA 02167 • 1 spec.; 23.6 mm SL; Bom Jesus do Tocantis, Jacundá River, Tocantins River basin; 5°15'1" S, 48°48'58" W; 21 Aug. 2017; E.C. Guimarães and P.S. Brito leg.; CICCAA 2348 • 5 specs; 21.1–23.1 mm SL (C&S); Marabá municipality, Flexeiras River, Tocantins River basin; 5°15'38" S, 48°59'35" W; 21 Aug. 2017; E.C. Guimarães and P.S. Brito leg.; CICCAA 04800 • 1 spec.; 17.9 mm SL; Bom Jesus do Tocantis, Jacundá River, Tocantins River basin; 5°15'1" S, 48°48'58" W; 21 Sep. 2018; E.C. Guimarães and P.S. Brito leg.; UFRJ 6919 • 4 specs; 16.3–19.2 mm SL; Marabá municipality, Tocantins River basin; 5°15'38" S, 48°59'35" W; 10 Jul. 2017; E.C. Guimarães and P.S. Brito leg.; CICCAA 01839 • 5 specs; 18.0–18.9 mm SL (C&S); Marabá municipality, Tocantins River basin; 5°15'38" S, 48°59'35" W; 21 Sep. 2018; E.C. Guimarães and P.S. Brito leg.; CICCAA 02402 – **Maranhão State** • 1 spec.; 26.1 mm SL; Igarapé Papagaio, Tocantins River basin; 5°8'59" S, 48°22'33" W; 20 Jan. 2014; E.C. Guimarães leg.; CICCAA 01958.

Type locality

Brazil, Pará State, Marabá municipality, Flexeiras River, Tocantins River basin, 5°15'38" S, 48°59'35" W (Fig. 3).

Description

Morphometric data of holotype and paratypes are presented in Table 3.

BODY. Small (with maximum SL of 23.6 mm), compressed, moderately deep, greatest body depth slightly anterior to dorsal-fin base; body profile straight and downward directed from end of dorsal fin to adipose fin, straight or slightly convex between latter point and origin of dorsal most procurrent caudal-fin ray; dorsal profile of head convex from upper lip to vertical through eye; predorsal profile of body roughly straight, dorsal-fin base slightly convex, posteroventrally inclined; ventral profile of head convex from lower jaw to pelvic-fin origin; straight and posterodorsally slanted along anal-fin base; and slightly concave on caudal peduncle; jaws equal, mouth terminal. Maxilla reaching vertical to anterior margin of pupil.

TEETH. Premaxillary teeth in two rows. Outer row with two tricuspid teeth; inner row with 5(2), 6(3) tricuspid teeth. Maxilla with 2(2), 3(2) or 4(1) pentacuspid teeth. Dentary with five (3) or six (2) larger tricuspid teeth followed by five (4) or six (1) smaller pentacuspid tooth (Fig. 6).

SCALES. Scales cycloid, three to eight radii strongly marked, circuli well-marked anteriorly, weakly-marked posteriorly; lateral line incompletely pored, with 7(31)* or 8(21) perforated scales. Longitudinal scales series including lateral-line scales 34(4), 35(2), 36(43)* or 37(1). Longitudinal scales rows between dorsal-fin origin and lateral line 5(46) or 6(4). Horizontal scale rows between lateral line and pelvic-fin origin 4(50) or 5(2). Scales in median series between tip of supraoccipital spine and dorsal-fin origin 9(35) or 10(15). Circumpeduncular scales 12(52).

FINS. Dorsal-fin origin at midbody. Base of last dorsal-fin ray at vertical through first third of anal fin. Dorsal-fin rays ii + 9(50)* or iii + 9(2). First dorsal-fin pterygiophore main body located behind neural spine of 4th vertebrae. Adipose fin present. Anal-fin origin aligned with vertical line through middle of dorsal fin, between 6th and 8th dorsal-fin rays. Anteriormost anal-fin pterygiophore inserting posterior to haemal spine of 11th vertebrae. Anal-fin origin aligned with vertical line through middle of dorsal fin (between base of 6th and 8th dorsal-fin rays). Anal fin iii + 22(40)* or iii + 23(12); Anterior anal-fin margin slightly convex, with anteriormost rays more elongate and slightly more thickened than remaining rays, forming a distinct lobe. Remaining rays smaller with straight distal margin. Pectoral-fin rays 12(52) total rays. Tip of pectoral fin surpassing pelvic-fin base. Pelvic-fin rays 8(52) total rays, surpassing anal-fin origin. Caudal fin forked, upper and lower lobes similar in size. Principal caudal-fin rays 11+10(30) or 10+9(22); dorsal procurrent rays 8(8) or 9(2) and ventral procurrent rays 7(3) or 8(7).

OSTEOLOGICAL COUNTS. Branchiostegal rays 10(10). First gill arch with 1(8), 2(2) hypobranchial, 11(2), 12(8) ceratobranchial, 1(10) cartilage between ceratobranchial and epibranchial, and 5(2) or 6(8) epibranchial gill-rakers. Supraneurals 4(8) or 5(2). Precaudal vertebrae 11 (10) and caudal vertebrae 19 (10). Total vertebrae 30(10).

Coloration in alcohol (Fig. 4)

Ground coloration light yellowish brown. Humeral spot conspicuous, slightly vertically elliptical, with a thin vertical line, formed by the concentration of dark chromatophores, at middle of humeral spot, extending one to two scales above and below humeral spot. Flank with conspicuous chromatophores scattered mainly on middle region, from just after humeral spot, reaching caudal peduncle end. Ventral region lacking dark brown chromatophores. Dark brown chromatophores present on head,

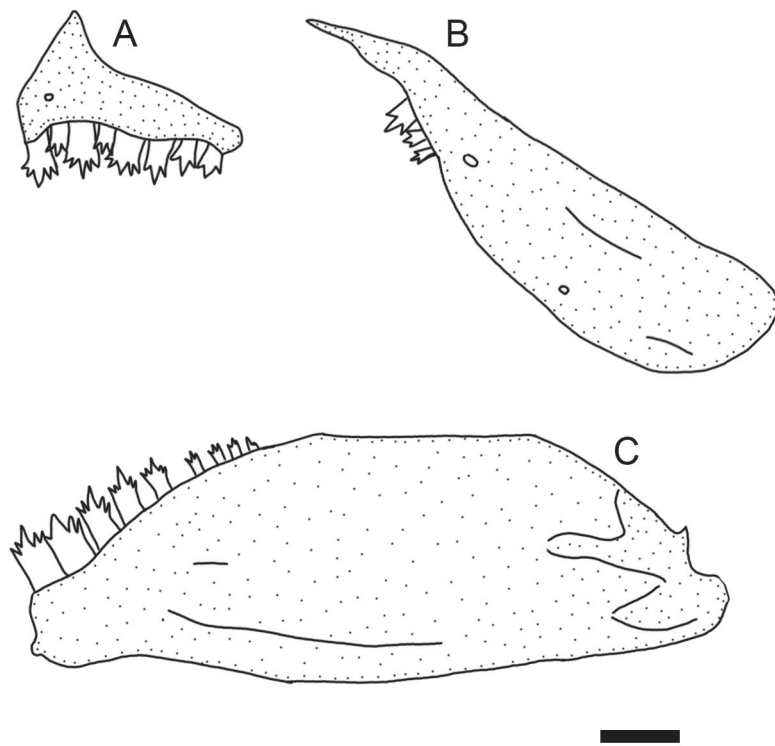


Fig. 6. *Hyphessobrycon geryi* Guimarães, Brito, Bragança, Katz & Ottoni sp. nov. (CICCAA 02402), 23.2 mm SL. Jaw suspensory. A. Premaxillary. B. Maxilla. C. Dentary. Scale bar: 1 mm

more concentrated on dorsal portion, tip of snout, and opercular region, becoming sparser on cheek. Dorsal-fin ground coloration hyaline, with conspicuous black or dark brown spot located on anterior portion of fin, reaching about 6th ray, approximately between half to two thirds of fin depth. Conspicuous pigmentation on dorsal-fin base formed by concentration of conspicuous chromatophores. Anal and caudal fins hyaline. Anal and caudal fin with darker, usually dark brown, posterior margin. Adipose fin hyaline to light brown, with dark chromatophores at margin and posterior portion. Pectoral and pelvic fins hyaline; pelvic fin with variable amounts of dark brown pigmentation remaining depending on specimen preservation state.

Color in life (Fig. 5)

Color pattern similar to coloration of preserved specimens, with more translucent body. Ground coloration translucent, white to grey, with orange pigmentation on vertebrae region, and usually with orange chromatophores. Ventral region anterior to anal-fin origin lighter.

Chromatophores on humeral region black. Head darker than flank, especially on opercular and dorsal regions; ventrally lighter. Conspicuous black spot on dorsal fin, with yellow or white pigmentation on dorsal and ventral margins of spot; rest of dorsal fin hyaline. Anal fin base with light red chromatophores, with different degrees of intensity, with milk white pigmentation on anterior tip of anal fin, reaching between first to second rays. Adipose fin hyaline, with light red chromatophores mainly at base, and black chromatophores at margin. Pectoral and pelvic fins hyaline, with some sparser dark brown chromatophores, more concentrated at pelvic fin, and with milk white pigmentation on anterior tip of pelvic fin. Caudal fin with red pigmentation on almost fin, with inconspicuous light brown margin.

Sexual dimorphism

Bony hooks on fins is absent in all examined specimens. According to Malabarba & Weitzman (2003) the presence of bony hooks is a common dimorphic feature among characids species. Although this sexual dimorphism is not observed in all characid species, as in case of species described here. Color pattern is not sexually dimorphic either.

Species delimitation

WP and CBB

The BI phylogenetic analysis supported a clade comprising *Hypessobrycon geryi* Guimarães, Brito, Bragança, Katz & Ottoni sp. nov., *H. copelandi*, *H. frickeyi* Guimarães, Brito, Bragança, Katz & Ottoni sp. nov. and *H. aff. copelandi*, hereafter termed *Hypessobrycon copelandi* clade, with maximum posterior probability value (posterior probability = 1). *Hypessobrycon frickeyi* sp. nov. and *H. geryi* sp. nov. haplotypes formed two exclusive clades with maximum posterior probability value (posterior probability = 1), as well as *H. copelandi* and *H. aff. copelandi*. The nucleotide substitutions supporting these lineages within the *H. copelandi* clade are presented in Fig. 7 and Appendix 2. The combination of nucleotide substitutions diagnosing *H. frickeyi* sp. nov. and *H. geryi* sp. nov. are presented in the molecular diagnosis section.

DBC

The alignment comprised a total of 26 haplotypes. After trimming, the final alignment yielded 639 base pairs with 159 polymorphic sites. Average genetic distances were 17%, with the highest values between *H. epicharis* and *H. erythrostigma* (23.4%), while the lowest value of (0.08%) was between *H. pyrrhonotus* and *H. erythrostigma* (Table 3). *Hypessobrycon frickeyi* sp. nov. and *H. geryi* sp. nov. are divergent on average 17%, from the other taxa, with a minimum distance of 3.5% and 4.4%, respectively, to *H. copelandi*, and 4.7% of divergence between them (Table 4), thus both species being recovered by this genetic distance method.

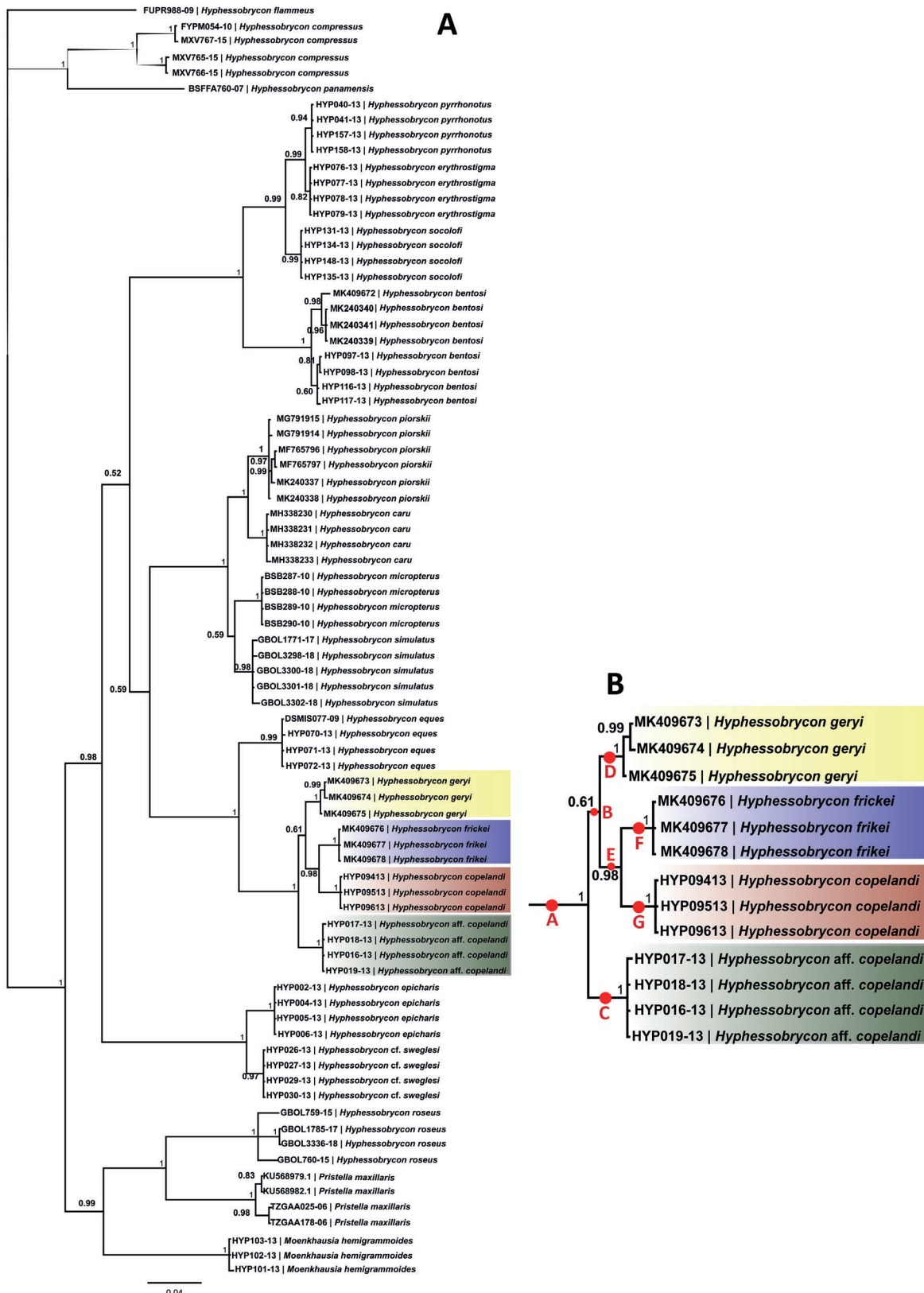


Fig. 7. **A.** Bayesian Inference phylogenetic tree (BI). **B.** Detached relationships between members of the *Hypessobrycon copelandi* clade. Numbers above and below branches are posterior probability values, and red letters correspond to synapomorphic nucleotide substitutions listed in Appendix 2.

GMYC and bPTP

Both unilocus coalescent species delimitation methods delimited the same eight lineages (species): *H. caru*, *H. piorskii*, *H. geryi* sp. nov., *H. copelandi*, *H. frickei* sp. nov. and *H. aff. copelandi*; in addition to the species included as outgroup, *H. bentosi*, that was split into two distinct lineages (Fig. 8).

ABDG

In the ABDG species delimitation method, the same ingroup taxa as delimited in the coalescent species delimitation methods have been defined comprising: *H. caru*, *H. piorskii*, *H. geryi* sp. nov., *H. copelandi*, *H. frickei* sp. nov. and *H. aff. copelandi*. In contrast to the coalescent methods results, all haplotypes from *H. bentosi*, the outgroup taxa, were recognized as a single species. The same seven groups (species) were delimited between P values ranging from 0.0017 and 0.0215 (Fig. 8).

Discussion

Recent DNA-based studies suggest that tropical faunas contain a large proportion of undescribed species (e.g., Roca *et al.* 2001; Hrbek *et al.* 2014; Poulakakis *et al.* 2015; Murphy *et al.* 2016; Bittencourt *et al.* 2019; Guimarães *et al.* 2018, 2019; de Brito *et al.* 2019). This fact is more evident in freshwater fishes, since freshwater systems are isolated, hampering the migration of species from one river system into another. Such a situation favors speciation, in many cases resulting in cryptic species, which is common among Neotropical fish lineages, as evidenced and revealed by work dealing with species delimitation molecular approaches (e.g., Costa & Amorim 2011; Costa *et al.* 2012, 2014, 2017; Pereira *et al.* 2011; Benzaquem *et al.* 2015; Melo *et al.* 2014, 2016a, 2016b, 2016c; Amorim 2018; Mattos & Costa 2018; Carvalho *et al.* 2018; Guimarães *et al.* 2018, 2019; Rosso *et al.* 2018; Ottoni *et al.* 2019; de Santana *et al.* 2019). Recently, the presence of cryptic species and a greater biodiversity have been also evidenced for the “Rosy tetra” clade (e.g., Castro-Paz *et al.* 2014; Guimarães *et al.* 2018, 2019), which is herein corroborated, with the description of two new species belonging to this clade, based on seven different species delimitations methods.

In the present research, we suggest a new clade within the “Rosy tetra”, the *Hyphessobrycon copelandi* clade, comprising four species: *Hyphessobrycon copelandi*, with its type locality at Tabatinga, Amazonas, Brazil, close to the border with Peru and Colombia (Eigenmann 1908); the two new species herein described, *Hyphessobrycon frickei* Guimarães, Brito, Bragança, Katz & Ottoni sp. nov. and *H. geryi* Guimarães, Brito, Bragança, Katz & Ottoni sp. nov. from the Maracaçumé River basin in northeastern Brazil and the middle Tocantins River basin in east Amazon, Brazil, respectively; and an undescribed species from the lower Rio Negro basin (here called *H. aff. copelandi*). The *Hyphessobrycon copelandi* clade was corroborated by maximum node support (see Fig. 7), as well as, by 25 synapomorphic nucleotide substitutions (see Fig. 7 and Appendix 2).

Hyphessobrycon frickei sp. nov. and *H. geryi* sp. nov. were identified as new species by seven different and independent methods of species delimitation (PAA, DBC, WP, CBB, bPTP, GMYC and ABGD), relying on different sources of characters (morphology and DNA), different criteria and assumptions; under an Integrative Taxonomy perspective (Systsma & Schaal 1985; Dayrat 2005; Goldstein & Desalle 2010; Padial *et al.* 2010). Both species are distinguished from all their congeners mainly by the arrangement, shape and color pattern of the humeral and dorsal-fin spots, as well as by other characters related to scale counts and body pigmentation (see PAA – Diagnosis). In our bayesian inference phylogenetic analysis (Fig. 7), haplotypes belonging to both species formed two exclusive clades with maximum posterior probability value (posterior probability = 1) (WP), as well as, the other two species within the *Hyphessobrycon copelandi* clade. Furthermore, the minimum COI genetic distance (DBC) of *Hyphessobrycon frickei* sp. nov. and *H. geryi* sp. nov. when compared to *H. copelandi* were 3.5% and 4.4%, respectively, and 4.7% of divergence between them (see Table 4). Considering this value,

Table 3. Morphometric data (N = 53) for the holotype and paratypes of *Hypessobrycon geryi* Guimarães, Brito, Bragança, Katz & Ottoni sp. nov. SD = Standard deviation.

	Holotype	Paratypes	Mean	SD
Standard length	28.2	15.9–26.1	19.7	–
Percentages of standard length				
Depth at dorsal-fin origin (body depth)	32.4	27.7–34.4	31.5	1.2
Snout to dorsal-fin origin	51.5	49.6–53.6	51.5	0.8
Snout to pectoral-fin origin	25.7	26.4–29.7	28.2	1.1
Snout to pelvic-fin origin	42.7	44.1–47.0	45.1	0.8
Snout to anal-fin origin	57.2	53.4–63.4	58.8	1.7
Caudal peduncle depth	9.8	7.0–11.3	9.8	0.9
Caudal peduncle length	11.3	8.3–12.8	10.2	1.0
Pectoral-fin length	19.2	14.8–22.18	19.7	1.6
Pelvic-fin length	17.0	14.4–20.1	16.2	1.4
Dorsal-fin base length	13.9	11.9–15.9	14.4	0.8
Dorsal-fin height	25.5	23.5–33.0	28.1	1.8
Anal-fin base length	31.3	30.2–34.6	32.7	1.2
Eye to dorsal-fin origin	37.4	34.5–39.2	36.7	0.9
Dorsal-fin origin to caudal-fin base	54.7	50.5–56.2	53.7	1.1
Head length	27.6	26.9–29.8	29.1	0.6
Percentages of head length				
Horizontal eye diameter	36.8	36.8–46.1	41.4	2.3
Snout length	20.9	19.5–26.3	22.8	1.7
Least interorbital width	27.1	25.5–33.3	28.8	1.1
Upper jaw length	32.4	30.2–37.7	33.2	2.6

Hypessobrycon frickei sp. nov. and *H. geryi* sp. nov. genetic divergence is greater than that commonly inferred by species delimitations among Neotropical fish species (2%) based on COI (Jacobina et al. 2018). Moreover, *Hypessobrycon frickei* and *H. geryi* sp. nov. were also molecularly diagnosed by synapomorphic nucleotide substitutions, as well as by an accessory combination of other nucleotide substitutions (see CBB – molecular diagnosis sections, Fig. 7 and Appendix 2). At last, both coalescent species delimitation methods (GMYC and bPTP) corroborated these two new species, as well as, the Automatic Barcode Gap Discovery (ABGD) (Fig. 8). The same result found by all the methods applied here only reinforces the hypothesis that these species are in fact new to science.

Similar results from previous studies (e.g., Castro-Paz et al. 2014; Guimarães et al. 2018, 2019) agree with our hypothesis of the existence of cryptic species within the “Rosy tetra” clade, and also suggests that its species diversity is still underestimated. We would like to highlight the paper published by Guimarães et al. (2018, 2019) that also proposed and evidenced a new subclade within the “Rosy tetra” clade, the *Hypessobrycon micropterus* clade, revealing the existence of cryptic species and a greater diversity than previously known within the group.

Table 4. Kimura-2 parameters pairwise genetic distances among species of *Hyphessobrycon* Durbin, 1908 of the “rosy tetra” clade. Species of the *Hyphessobrycon copelandi* clade in bold.

		1	2	3	4	5	6	7	8	9	10	11	12	13	14	15	16
1	<i>H. bentosi</i>																
2	<i>H. compressus</i>	0.216															
3	<i>H. cf. sweglesi</i>	0.219	0.214														
4	<i>H. roseus</i>	0.216	0.208	0.217													
5	<i>H. epicharis</i>	0.225	0.217	0.033	0.213												
6	<i>H. erythrostigma</i>	0.104	0.219	0.206	0.219	0.233											
7	<i>H. pyrrhonotus</i>	0.098	0.219	0.201	0.223	0.230	0.008										
8	<i>H. socoloifi</i>	0.108	0.220	0.200	0.192	0.226	0.038	0.038									
9	<i>H. micropterus</i>	0.186	0.213	0.182	0.210	0.174	0.201	0.196	0.195								
10	<i>H. simulatus</i>	0.182	0.209	0.182	0.183	0.179	0.189	0.188	0.178	0.045							
11	<i>H. caru</i>	0.194	0.210	0.207	0.204	0.193	0.202	0.202	0.199	0.055	0.060						
12	<i>H. piorskii</i>	0.200	0.205	0.205	0.195	0.197	0.190	0.185	0.186	0.069	0.066	0.042					
13	<i>H. eques</i>	0.201	0.211	0.199	0.182	0.198	0.185	0.191	0.168	0.164	0.162	0.170	0.164				
14	<i>H. aff. copelandi</i>	0.208	0.198	0.220	0.195	0.209	0.188	0.185	0.182	0.187	0.183	0.173	0.168	0.102			
15	<i>H. geryi</i> sp. nov.	0.205	0.206	0.209	0.196	0.195	0.194	0.191	0.190	0.185	0.185	0.171	0.176	0.097	0.041		
16	<i>H. frickei</i> sp. nov.	0.208	0.218	0.212	0.210	0.204	0.193	0.190	0.187	0.171	0.167	0.166	0.160	0.099	0.060	0.047	
17	<i>H. copelandi</i>	0.220	0.213	0.211	0.209	0.202	0.201	0.198	0.190	0.181	0.176	0.173	0.168	0.106	0.058	0.044	0.035

Conclusion

The present paper highlights the importance of a species delimitation through an integrative framework allowing to solve taxonomic and classification problems in *Hypessobrycon* taxonomy, and estimating the diversity of this group with accuracy, being crucial for future studies on phylogeny, phylogeography, ecology, conservation and biogeography. We consider that difficulties to recognize the boundaries at the species or genus levels can be overcome through the adoption of integrative studies and perspectives, dealing with multiple criteria and character sources to make taxonomic decisions.

Acknowledgements

Thanks are owed to A. Zarske, I. Schindler, O. Lasso-Alcalá and R. Fricke for providing useful literature; Vale S.A and Amplo Engenharia for the cession of part of the data analyzed in this study; Raphael Covain (MHNG) and collaborators of the Project Gui-BOL Barcoding Guianese fishes for the cession of part

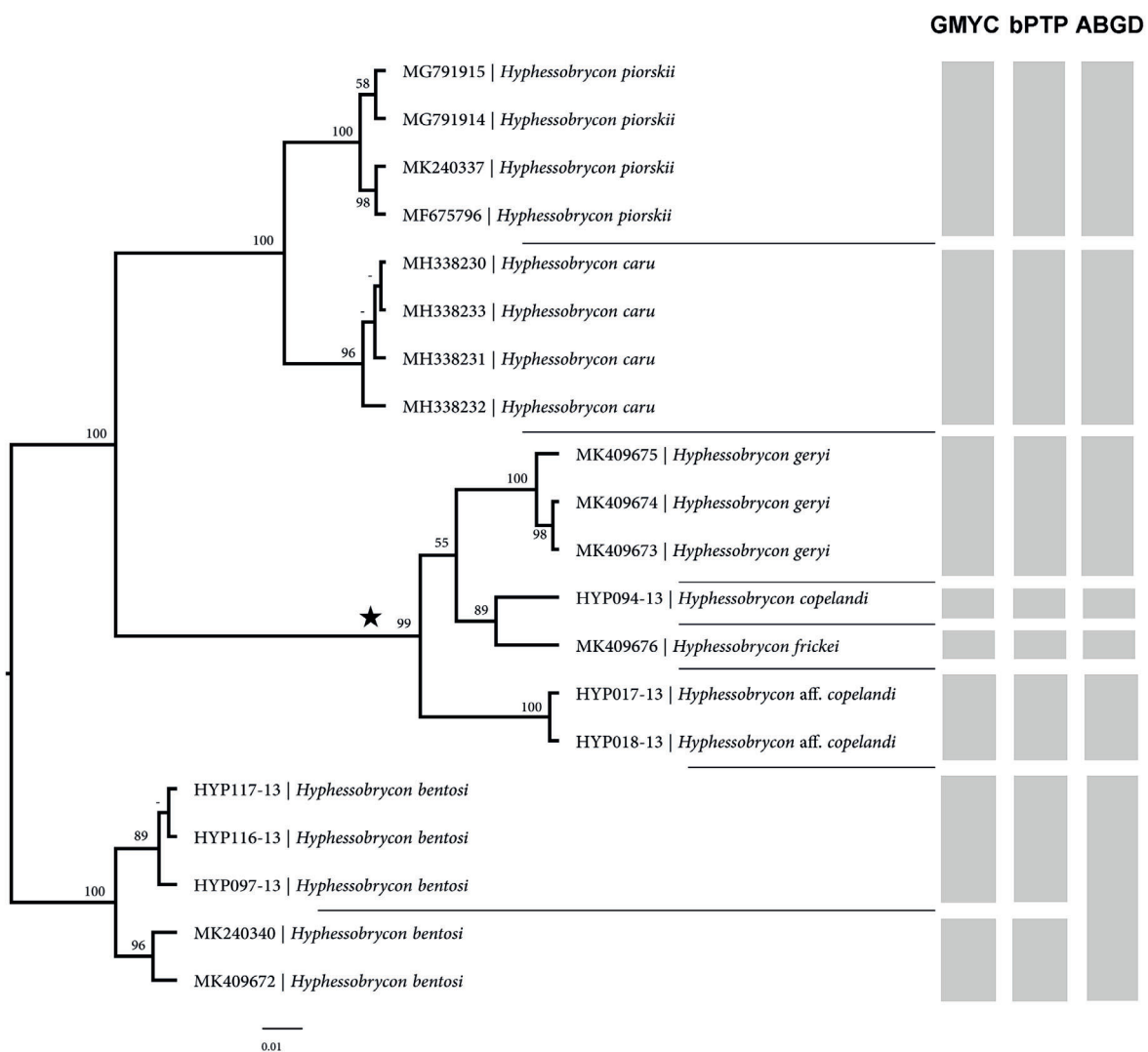


Fig. 8. Topology of the ultrametric tree performed in BEAST ver. 1.8.4 including unique haplotypes summarizing the results of GMYC, bPTP and ABGD. Numbers above and below branches are posterior probability values. The star indicates the *Hypessobrycon copelandi* clade.

of the data analyzed in this study; Wilson Costa (UFRJ) for the loan and donation of material; Andrew Williston (MCZ), James MacLaine and Kevin Swagel (BMNH), Mark Sabaj Pérez and Dave Catania (CAS), Riedel Bettina (NMW) and Sandra Raredon (USNM) for providing photographs, x-ray images, and information on the type material of some species; CAPES (Coordenação de Aperfeiçoamento de pessoal de nível Superior - Finance Code 001) and FAPEMA for providing the scholarship to PSB under the process 88887.159561/2017-00. All material was collected with permits 51540-3/ from SISBIO (Brazilian Institute of Environment and Natural Resources).

References

- Alfaro M.E. & Holder M.T. 2006. The posterior and the prior in Bayesian phylogenetics. *Annual Review of Ecology, Evolution, and Systematics* 37: 19–42.
<https://doi.org/10.1146/annurev.ecolsys.37.091305.110021>
- Amorim F.P. 2018. *Jenynsia lineata* species complex, revision and new species description (Cyprinodontiformes: Anablepidae). *Journal of Fish Biology* 92: 1312–1332.
<https://doi.org/10.1111/jfb.13587>
- Avise J.C. 2000. *Phylogeography: the History on Formation of Species*. University Press, Cambridge.
- Benine R.C., Melo B.F., Castro R.M.C. & Oliveira C. 2015. Taxonomic revision and molecular phylogeny of *Gymnocorymbus* Eigenmann, 1908 (Teleostei, Characiformes, Characidae). *Zootaxa* 3956 (1): 1–28. <https://doi.org/10.11646/zootaxa.3956.1.1>
- Betancur-R R., Arcila D., Vari R.P., Hughes L.C., Oliveira C., Sabaj M.H. & Ortí G. 2018. Phylogenomic incongruence, hypothesis testing, and taxonomic sampling: The monophyly of characiform fishes. *Evolution* 73 (2): 329–345. <https://doi.org/10.1111/evol.13649>
- Benzaquem D.C., Oliveira C., da Silva Batista J., Zuanon J. & Porto J.I.R. 2015. DNA Barcoding in Pencilfishes (Lebiasinidae: *Nannostomus*) Reveals Cryptic Diversity across the Brazilian Amazon. *PLoS ONE* 10 (2): e0112217. <https://doi.org/10.1371/journal.pone.0112217>
- Bickford D., Lohman D.J., Sodhi N.S., Ng P.K.L., Meier R., Winker K., Ingram K.K. & Das I. 2006. Cryptic species as a window on diversity and conservation. *Trends in Ecology and Evolution* 22 (3): 148–155. <https://doi.org/10.1016/j.tree.2006.11.004>
- Bittencourt P.S., Campos Z., Muniz F.L., Marioni B., Souza B.C., Da Silveira R., de Thoisy B., Hrbek T. & Farias I.P. 2019. Evidence of cryptic lineages within a small South American crocodilian: the Schneider's dwarf caiman *Paleosuchus trigonatus* (Alligatoridae: Caimaninae). *PeerJ* 7: e6580. <https://doi.org/10.7717/peerj.6580>
- Bragança P.H.N., Ottoni F.P. & Rangel-Pereira F.S. 2015. *Hyphessobrycon ellisae*, a new species from northeastern Brazil (Teleostei: Characidae). *Ichthyological Exploration of Freshwaters* 26 (3): 255–262.
- de Brito P.S., Guimarães E.C., Carvalho-Costa L.F. & Ottoni F.P. 2019. A new species of *Aphyocharax* Günther, 1868 (Characiformes, Characidae) from the Maracaçumé river basin, eastern Amazon. *Zoosystematics and Evolution* 95 (2): 507–516. <https://doi.org/10.3897/zse.95.36788>
- Carvalho F.R. & Malabarba L.R. 2015. Redescription and osteology of *Hyphessobrycon compressus* (Meek) (Teleostei: Characidae), type species of the genus. *Neotropical Ichthyology* 13 (3): 513–540. <https://doi.org/10.1590/1982-0224-20140173>
- Carvalho M.L., Costa Silva G.J., Melo S., Ashikaga F.Y., Shimabukuro-Dias C.K., Scacchetti P.C., Devidé R., Foresti F. & Oliveira C. 2018. The non-monotypic status of the neotropical fish genus *Hemiodontichthys* (Siluriformes, Loricariidae) evidenced by genetic approaches. *Mitochondrial DNA Part A* 29 (8): 1224–1230. <https://doi.org/10.1080/24701394.2018.1431230>

Castro-Paz F.P., Batista J.S. & Porto J.I.R. 2014. DNA Barcodes of Rosy Tetras and Allied Species (Characiformes: Characidae: *Hyphe**sobrycon*) from the Brazilian Amazon Basin. *PLoS ONE* 9 (5): e98603. <https://doi.org/10.1371/journal.pone.0098603>

Chenna R., Sugawara H., Koike T., Lopez R., Gibson T.J., Higgins D.G. & Thompson J.D. 2003. Multiple sequence alignment with the Clustal series of programs. *Nucleic Acids Research* 31: 3497–3500. <https://doi.org/10.1093/nar/gkg500>

Close B., Banister K., Baumans V., Bernoth E.M., Bromage N., Bunyan J., Erhardt W., Flecknell P., Gregory N., Hackbarth H. & Morton D. 1996. Recommendations for euthanasia of experimental animals: Part 1. *Laboratory Animals* 30 (4): 293e316. <https://doi.org/10.1258/002367796780739871>

Close, B., Banister, K., Baumans, V., Bernoth, E.M., Bromage, N., Bunyan, J., Erhardt, W., Flecknell, P., Gregory, N., Hackbarth, H. & Morton, D. 1997. Recommendations for euthanasia of experimental animals: Part 2. *Laboratory Animals* 31 (1): 1e32. <https://doi.org/10.1258/002367797780600297>

Costa W.J.E.M. & Amorim P.F. 2011. A new annual killifish species of the *Hypselebias flavicaudatus* complex from the São Francisco River basin, Brazilian Caatinga (Cyprinodontiformes: Rivulidae). *Vertebrate Zoology* 61 (1): 99–104.

Costa W.J.E.M., Amorim P.F. & Mattos J.L.O. 2012. Species delimitation in annual killifishes from the Brazilian Caatinga, the *Hypselebias flavicaudatus* complex (Cyprinodontiformes: Rivulidae): implications for taxonomy and conservation. *Systematics and Biodiversity* 10: 71–91. <https://doi.org/10.1080/14772000.2012.664177>

Costa W.J.E.M., Amorim P.F. & Aranha G.N. 2014. Species limits and DNA barcodes in *Nematolebias*, a genus of seasonal killifishes threatened with extinction from the Atlantic Forest of south-eastern Brazil, with description of a new species (Teleostei: Rivulidae). *Ichthyological Exploration of Freshwaters* 24 (3): 225–236.

Costa W.J.E.M., Cheffe M.M. & Amorim P.F. 2017. Two new seasonal killifishes of the *Austrolebias adloffii* group from the Lagoa dos Patos basin, southern Brazil (Cyprinodontiformes: Aplocheilidae). *Vertebrate Zoology* 67 (2): 139–149.

Darriba D., Taboada G.L., Doallo R. & Posada D. 2012. jModelTest 2: more models, new heuristics and parallel computing. *Nature Method* 9 (8): 772. <https://doi.org/10.1038/nmeth.2109>

Davis J.I. & Nixon K.C. 1992. Populations, genetic variation, and the delimitation of phylogenetics species. *Systematic Biology* 41 (4): 421–435. <https://doi.org/10.1093/sysbio/41.4.421>

Dayrat B. 2005. Towards integrative taxonomy. *Biological Journal of the Linnean Society* 85 (3): 407–415. <https://doi.org/10.1111/j.1095-8312.2005.00503.x>

Desalle R., Egan M.G. & Siddall M. 2005. The unholy trinity: taxonomy, species delimitation and DNA barcoding. *Philosophical Transactions of the Royal Society B* 360: 1905–1916. <https://doi.org/10.1098/rstb.2005.1722>

Drummond A.J., Suchard M.A., Xie D. & Rambaut A. 2012. Bayesian phylogenetics with BEAUti and the BEAST 1.7. *Molecular Biology and Evolution* 29: 1969–1973.

Eigenmann C.H. 1908. Preliminary descriptions of new genera and species of Tetragonopterid characins. *Bulletin of the Museum of Comparative Zoology* 52: 91–106.

Eigenmann C.H. 1918. The American Characidae (Part 2). *Memoirs of the Museum of Comparative Zoology* 43: 101–208.

Fink W. & Weitzman S. 1974. The so called cheirodontin fishes of Central America with descriptions of two new species (Pisces: Characidae). *Smithsonian Contributions to Zoology* 172: 1–45.

<https://doi.org/10.5479/si.00810282.172>

Fricke R. & Eschmeyer W.N. 2020. Guide to fish collections.

Available from <http://researcharchive.calacademy.org/research/ichthyology/catalog/collections.asp> [accessed 10 Mar. 2020].

Fricke R., Eschmeyer W.N. & van der Laan R. 2020a. Catalog of Fishes: Genera, Species, References. Available from <http://researcharchive.calacademy.org> [accessed 31 Mar. 2020].

Fricke R., Eschmeyer W.N. & Jon D.F. 2020b. Catalog of Fishes: Species by Family/Subfamily.

Available from

<http://researcharchive.calacademy.org/research/ichthyology/catalog/SpeciesByFamily.asp> [accessed 31 Mar. 2020].

Fujisawa T. & Barraclough T.G. 2013. Delimiting species using single-locus data and the Generalized Mixed Yule Coalescent approach: a revised method and evaluation on simulated datasets. *Systematic Biology* 62 (5): 707–724. <https://doi.org/10.1093/sysbio/syt033>

García-Alzate C.A., Román-Valencia C. & Taphorn D.C. 2008. Revision of the *Hyphessobrycon heterorhabdus*-group (Teleostei: Characiformes: Characidae), with description of two new species from Venezuela. *Vertebrate Zoology* 58 (2): 139–157.

García-Melo J.E., Oliveira C., Da Costa Silva G.J., Ochoa-Orrego L.E., Garcia Pereira L.H. & Maldonado-Ocampo J.A. 2019. Species delimitation of neotropical Characins (Stevardiinae): Implications for taxonomy of complex groups. *PLoS ONE* 14 (6): e0216786.

<https://doi.org/10.1371/journal.pone.0216786>

Géry J. 1977. *Characoids of the World*. TFH-publications, Neptune City Inc.

Goldstein P.Z. & Desalle R. 2010. Integrating DNA barcode data and taxonomic practice: determination, discovery, and description. *BioEssays* 33 (2): 135–147. <https://doi.org/10.1002/bies.201000036>

Guimarães E.C., De Brito P.S., Feitosa L.M., Carvalho-Costa L.F. & Ottoni F.P. 2018. A new species of *Hyphessobrycon* Durbin from northeastern Brazil: evidence from morphological data and DNA barcoding (Characiformes, Characidae). *ZooKeys* 765: 79–101. <https://doi.org/10.3897/zookeys.765.23157>

Guimarães E.C., De Brito P.S., Feitosa L.M., Carvalho-Costa L.F. & Ottoni F.P. 2019. A new cryptic species of *Hyphessobrycon* Durbin, 1908 (Characiformes, Characidae) from the Eastern Amazon, revealed by integrative taxonomy. *Zoosystematics and Evolution* 95 (2): 345–360.

<https://doi.org/10.3897/zse.95.34069>

Hebert P.D.N., Cywinski A., Ball S.L. & de Waard J.R. 2003a. Biological identifications through DNA barcodes. *Proceedings of the Royal Society B* 270(1512): 313–321. <https://doi.org/10.1098/rspb.2002.2218>

Hebert P.D.N., Ratnasingham S. & de Waard J.R. 2003b. Barcoding animal life: cytochrome c oxidase subunit 1 divergences among closely related species. *Proceedings of the Royal Society B* 270 (1): 96–99. <https://doi.org/10.1098/rsbl.2003.0025>

Hebert P.D.N., Penton E.H., Burns J.M., Janzen D.H. & Hallwachs W. 2004a. Ten species in one: DNA barcoding reveals cryptic species in the neotropical skipper butterfly *Astraptes fulgerator*. *Proceedings of the National Academy of Sciences* 101 (41): 14812–14817. <https://doi.org/10.1073/pnas.0406166101>

Hebert P.D.N., Stoeckle M.Y., Zemlak T.S. & Francis C.M. 2004b. Identification of birds through DNA barcodes. *PLoS Biology* 2 (10): e312. <https://doi.org/10.1371/journal.pbio.0020312>

Hrbek T., Da Silva V.M.F., Dutra N., Gravena W., Martin A.R. & Farias I.P. 2014. A new species of river dolphin from Brazil or: How little do we know our biodiversity. *PLoS ONE* 9 (1): e83623.

<https://doi.org/10.1371/journal.pone.0083623>

- Huelsenbeck J.P. & Ronquist F. 2001. Mr. Bayes: Bayesian inference of phylogenetic trees. *Bioinformatics* 17 (8): 754–755. <https://doi.org/10.1093/bioinformatics/17.8.754>
- Jacobina U.P., Lima S.M.Q., Maia D.G., Souza G., Batalha-Filho H. & Torres R.A. 2018. DNA barcode sheds light on systematics and evolution of neotropical freshwater trahiras. *Genetica* 146 (6): 505–515. <https://doi.org/10.1007/s10709-018-0043-x>
- Javonillo R., Malabarba L.R., Weitzman S.H. & J.R. Burns. 2010. Relationships among major lineages of characid fishes (Teleostei: Ostariophysi: Characiformes), based on molecular sequence data. *Molecular Phylogenetics and Evolution* 54 (2): 498–511. <https://doi.org/10.1016/j.ympev.2009.08.026>
- Kimura M. 1980. A simple method for estimating evolutionary rates of base substitutions through comparative studies of nucleotide sequences. *Journal of Molecular Evolution* 16 (2): 111–120. <https://doi.org/10.1007/BF01731581>
- Kumar S., Stecher G. & Tamura K. 2016. MEGA7: Molecular evolutionary genetics analysis version 7.0 for bigger datasets. *Molecular Biology and Evolution* 33: 1870–1874. <https://doi.org/10.1093/molbev/msw054>
- Leary S., Underwood W., Anthony R., Cartner S., Corey D. & Grandin T. 2013. AVMA Guidelines for the Euthanasia of Animals. Available from: http://works.bepress.com/cheryl_greenacre/14 [accessed 31 Mar. 2020].
- Malabarba L. R. & Weitzman S. H. 2003. Description of a new genus with six new species from Southern Brazil, Uruguay and Argentina, with a discussion of a putative characid clade (Teleostei: Characiformes: Characidae). *Comunicações do Museu de Ciências e Tecnologia, PUCRS, Série Zoologia* 16 (1): 67–151.
- Mattos J.L.O. & Costa W.J.E.M. 2018. Three new species of the ‘*Geophagus*’ *brasiliensis* species group from the northeast Brazil (Cichlidae, Geophagini). *Zoosystematics and Evolution* 94 (2): 325–337. <https://doi.org/10.3897/zse.94.22685>
- Melo B.F., Sidlauskas B.L., Hoekzema K., Vari R.P. & Oliveira C. 2014. The first molecular phylogeny of Chilodontidae (Teleostei: Ostariophysi: Characiformes) reveals cryptic biodiversity and taxonomic uncertainty. *Molecular Phylogenetics and Evolution* 70: 286–295. <https://doi.org/10.1016/j.ympev.2013.09.025>
- Melo B.F., Ochoa L.E., Vari R.P. & Oliveira C. 2016a. Cryptic species in the Neotropical fish genus *Curimatopsis* (Teleostei, Characiformes). *Zoologica Scripta* 45: 650–658. <https://doi.org/10.1111/zsc.12178>
- Melo B.F., Sidlauskas B.L., Hoekzema K., Frable B.W., Vari R.P. & Oliveira C. 2016b. Molecular phylogenetics of the Neotropical fish family Prochilodontidae (Teleostei: Characiformes). *Molecular Phylogenetics and Evolution* 102: 189–201. <https://doi.org/10.1016/j.ympev.2016.05.037>
- Melo B.F., Benine R.C., Silva G.S.C., Avelino G.S. & Oliveira C. 2016c. Molecular phylogeny of the Neotropical fish genus *Tetragonopterus* (Teleostei: Characiformes: Characidae). *Molecular Phylogenetics and Evolution* 94: 709–717. <https://doi.org/10.1016/j.ympev.2015.10.022>
- Mirande J.M. 2010. Phylogeny of the family Characidae (Teleostei: Characiformes): from characters to taxonomy. *Neotropical Ichthyology* 8 (3): 385–568. <https://doi.org/10.1590/S1679-62252010000300001>
- Mirande J.M. 2018. Morphology, molecules and the phylogeny of Characidae (Teleostei, Characiformes). *Cladistics* 1–19. <https://doi.org/10.1111/cla.12345>
- Murphy J.C., Jowers M.J., Lehtinen R.M., Charles S.P., Colli G.R., Peres Jr.A.K., Hendry C.R. & Pyron R.A. 2016. Cryptic, sympatric diversity in tegu lizards of the *Tupinambis teguixin* group (Squamata, Sauria, Teiidae) and the description of three new species. *PLoS ONE* 11 (8): e0158542.

<https://doi.org/10.1371/journal.pone.0158542>

Oliveira C., Avelino G.S., Abe K.T., Mariguela T.C., Benine R.C., Ortí G., Vari R.P. & Castro R.M.C. 2011. Phylogenetic relationships within the speciose family Characidae (Teleostei: Ostariophysi: Characiformes) based on multilocus analysis and extensive ingroup sampling. *BMC Evolutionary Biology*, 11, 275. <https://doi.org/10.1186/1471-2148-11-275>

Ota R.R., Carvalho F.R. & Pavanelli C.S. 2020. Taxonomic review of the *Hyphephessobrycon panamensis* species-group (Characiformes: Characidae). *Zootaxa* 4751 (3): 401–436.
<https://doi.org/10.11646/zootaxa.4751.3.1>

Ottone F.P., Mattos J.L.O., Katz A.M. & Braga P.H.N. 2019. Phylogeny and species delimitation based on molecular approaches on the species of the *Australoheros auratus* group (Teleostei, Cichlidae), with biogeographic comments. *Zoosystematics and Evolution* 95 (1): 49–64.
<https://doi.org/10.3897/zse.95.31658>

Padial J.M., Miralles A., De la Riva I. & Vences M. 2010. The integrative future of taxonomy. *Frontiers in Zoology* 7: 16. <https://doi.org/10.1186/1742-9994-7-16>

Pereira L.H.G., Pazian M.F., Hanner R., Foresti F. & Oliveira C. 2011. DNA barcoding reveals hidden diversity in the Neotropical freshwater fish *Piabina argentea* (Characiformes: Characidae) from the Upper Paraná basin of Brazil. *Mitochondrial DNA* 22 (1): 87–96.
<https://doi.org/10.3109/19401736.2011.588213>

Poulakakis N., Edwards D.L., Chiari Y., Garrick R.C., Russello M.A., Benavides E., Watkins-Colwell G.J., Glaberman S., Tapia W., Gibbs J.P., Cayot L.J. & Caccone A. 2015. Description of a new Galapagos giant tortoise species (Chelonioidae: Testudinidae) from Cerro Fatal on Santa Cruz Island. *PLoS ONE* 10 (10): e013877. <https://doi.org/10.1371/journal.pone.013877>

Puillandre N., Lambert A., Brouillet S. & Achaz G. 2012. ABGD, automatic barcode gap discovery for primary species delimitation. *Molecular Ecology* 21: 1864–1877.
<https://doi.org/10.1111/j.1365-294X.2011.05239.x>

Queiroz de K. 2005. Different species problems and their resolution. *BioEssays* 27 (12): 1263–1269.
<https://doi.org/10.1002/bies.20325>

Queiroz de K. 2007. Species concepts and species delimitation. *Systematic Biology* 56 (6): 879–886.
<https://doi.org/10.1080/10635150701701083>

Roca A.L., Georgiadis N.J., Pecon-Slattery J. & O'Brien S.J. 2001. Genetic evidence for two species of elephant in Africa. *Science* 80 (293): 1473–1477. <https://doi.org/10.1126/science.1059936>

Rosso J.J., González-Castro M., Bogan S., Cardoso Y.P., Mabragaña E., Delpiani M. & Astarloa J.M.D. 2018. Integrative taxonomy reveals a new species of the *Hoplias malabaricus* species complex (Teleostei: Erythrinidae). *Ichthyological Exploration of Freshwaters* IEF-1076: 1–18.
<https://doi.org/10.23788/IEF-1076>

Rozas J., Sánchez J.C., Messeguer X. & Rozas R. 2003. DnaSP, DNA polymorphism analyses by the 506 coalescent and other methods. *Bioinformatics* 19: 2496–2497.
<https://doi.org/10.1093/bioinformatics/btg359>

de Santana C.D., Crampton W.G., Dillman C.B., Frederico R.G., Sabaj M.H., Covain R., Ready J., Zuanon J., Oliveira R.R., Mendes Júnior R.N.G., Bastos D.A., Teixeira T.F., Mol J., Ohara W., Castro N.C., Peixoto L.A., Nagamachi C., Sousa L., Montag L.F.A., Ribeiro F., Waddell J.C., Piorsky N.M., Vari R.P. & Wosiacki W.B. 2019. Unexpected species diversity in electric eels with a description of the strongest living bioelectricity generator. *Nature Communications* 10: 4000.
<https://doi.org/10.1038/s41467-019-11690-z>

- Sites J.W. & Marshall J.C. 2003. Delimiting species: A Renaissance issue in systematic biology. *Trends in Ecology and Evolution* 18: 462–470. [https://doi.org/10.1016/S0169-5347\(03\)00184-8](https://doi.org/10.1016/S0169-5347(03)00184-8)
- Swofford D.L. 2002. PAUP. *Phylogenetic Analysis Using Parsimony (*and Other Methods)*, 4.0 edn, Sinauer, Sunderland, MA.
- Sytsma K.J. & Schaal B.A. 1985. Phylogenetics of the *Lisianthius skinneri* (Gentianaceae) complex in Panama utilizing DNA restriction fragment analysis. *Evolution* 39: 594–608.
- Taylor W.R. & Van Dyke G.C. 1985. Revised procedures for staining and clearing small fishes and other vertebrates for bone and cartilage study. *Cybium* 9 (2): 107–120.
- Ward R.D., Zemlak T.S., Innes B.H., Las, P.R. & Hebert P.D.N. 2005. DNA barcoding Australia's fish species. *Philosophical Transactions of the Royal Society of London B, Biological Sciences* 360 (1462): 1847–1857. <https://doi.org/10.1098/rstb.2005.1716>
- Weitzman S.H. 1962. The osteology of *Brycon meeki*, a generalized characid fish, with an osteological definition of the family. *Stanford Ichthyological Bulletin* 8 (1): 3–77.
- Weitzman S.H. & Palmer L. 1997. A new species of *Hyphessobrycon* (Teleostei: Characidae) from the Neblina region of Venezuela and Brazil, with comments on the putative ‘rosy tetra clade’. *Ichthyological Exploration of Freshwaters* 7 (3): 209–242.
- Wiens J.J. & Penkrot T.A. 2002. Delimiting species using DNA and Morphological variation and discordant limits in spiny lizards (*Sceloporus*). *Systematic biology* 51 (1): 69–91. <https://doi.org/10.1080/106351502753475880>
- Xia X.H. 2013. Dambe5: a comprehensive software package for data analysis in molecular biology and evolution. *Molecular Biology and Evolution* 30: 1720–1728. <https://doi.org/10.1093/molbev/mst064>
- Xia X.H., Xie Z., Salemi M., Chen L. & Wang Y. 2003. An index of substitution saturation and its application. *Molecular Phylogenetics and Evolution* 26: 1–7. [https://doi.org/10.1016/S1055-7903\(02\)00326-3](https://doi.org/10.1016/S1055-7903(02)00326-3)
- Zhang J., Kapli P., Pavlidis P. & Stamatakis A. 2013. A general species delimitation method with applications to phylogenetic placements. *Bioinformatics* 29: 2869–2876. <https://doi.org/10.1093/bioinformatics/btt499>

Manuscript received: 27 April 2020

Manuscript accepted: 28 July 2020

Published on: 9 November 2020

Topic editor: Rudy Jocqué

Desk editor: Marianne Salaün

Printed versions of all papers are also deposited in the libraries of the institutes that are members of the *EJT* consortium: Muséum national d'histoire naturelle, Paris, France; Botanic Garden Meise, Belgium; Royal Museum for Central Africa, Tervuren, Belgium; Royal Belgian Institute of Natural Sciences, Brussels, Belgium; Natural History Museum of Denmark, Copenhagen, Denmark; Naturalis Biodiversity Center, Leiden, the Netherlands; Museo Nacional de Ciencias Naturales-CSIC, Madrid, Spain; Real Jardín Botánico de Madrid CSIC, Spain; Zoological Research Museum Alexander Koenig, Bonn, Germany; National Museum, Prague, Czech Republic.

Appendix 1. Comparative material.

***H. bentosi*:** MCZ 20842, 15 specs (syntypes); USNM 120270, 3 specs (syntypes); CAS 42682, 3 specs (syntypes), Óbidos; CICCAA 04788, 100, specs, Óbidos municipality, Amazon River basin, Pará state, Brazil; CICCAA 04789, 30 specs (C&S) specs, Óbidos municipality, Amazon River basin, Pará state, Brazil. CICCAA 04790, 131, specs, Óbidos municipality, Amazon River basin, Pará state, Brazil. – ***H. caru*:** CICCAA 02286, 1 spec. (holotype); CICCAA 00706, 37 specs (paratypes); CICCAA 0709, 12 specs (C&S) (paratypes); LIOP.UFAM 1009, 1 spec. (paratypes), CICCAA00707, 3 specs (paratypes); CICCAA 00708, 2 specs (paratypes); UFRJ11745, 1 spec. (paratypes), Buriticupu municipality, Buritizinho River, Mearim River basin, Maranhão state, Brazil. – ***H. compressus*:** BMNH 1905.12.6.4–5, 2 specs (paratypes), Oaxaca state, México. – ***H. copelandi*:** CAS 42683, 5 specs (syntypes); MCZ 20771, 88 specs (syntypes); USNM 120271, 6 spms (syntypes), Tabatinga. CICCAA04834, 18 specs, Óbidos municipality, Amazon River basin, Pará state, Brazil. – ***H. eques*:** MMW 95056, 1 spec. (lectotype); NMW 62693, 6 specs (Paralectotypes); NMW59810, 2 specs (paralectotypes), Villa Bela, Óbidos; CICCAA 00715, 4 specs (C&S); CICCAA 00710, 51 specs, Tombos municipality, Paraíba do Sul River basin, Minas Gerais state, Brazil; CICCAA 00300, 24 specs; CICCAA 00699, 7 specs, Itaberaba municipality, São Francisco River basin, Bahia state, Brazil; CICCAA03447, 5 spmcs; CICCAA03448, 6 specs, Corumbá municipality, Paraguay River basin, Mato Grosso do Sul state, Brazil. CICCAA 04791, 240; CICCAA04792, 30 specs (C&S); CICCAA04793, 6 spmcs, Santarém municipality, Tapajós River basin, Pará State, Brazil. – ***H. erythrostigma*:** ANSP 70208, 1 spec. (holotype), Peru and Brazil. – ***H. epicharis*:** FMNH100609, 1 spec. (paratypes), Baria River, Amazonas, Venezuela. – ***H. haraldschultzi*:** CICCAA 00873, 20 specs, Ilha do Bananal municipality, Javaés River, Tocantins state, Brazil. – ***H. hasemani*:** ANSP 39230, 1 spec. (holotype), Guajaramirim municipality, Madeira River, Rondônia state, Brazil. – ***H. jackrobertsi*:** MTD F 33042, 1 spec. (holotype), Peru, vermutlich Umgebung von Iquitos; MTD F 33043-33051, 9 spmcs, Peru, vermutlich Umgebung von Iquitos; MTD F 33149-33158, 10 specs, Peru, Loreto, río Pastaza, río Chuinda, Lago de Rimachi. – ***H. micropterus*:** FMNHH 57916, 1 spec. (holotype), Lagoa de Porto, Minas Gerais state, Brazil. FMNH 57917, 14 specs (paratypes) Lagoa de Porto; FMNH 57918, 9 specs (paratypes); Santa Rita, São Francisco River basin; FMNH 57920, 25 specs (paratypes), Pirapora; FMNH 57920, 1 spec. (paratypes), Rio Salitre; FMNH 57921, 4 spec. (paratypes), Boqueirao, near mouth of Rio Preto. – ***H. paepkei*:** MTD F 33023, 1 spec. (holotype), Brasilien, Umgebung von Manaus. – ***H. piorskii*:** CICCAA 00695, 1 spec. (holotype); CICCAA 00430, 15 specs (paratypes); CICCAA 00431, 21 specs (paratypes); CICCAA 00696, 15 specs (paratypes); CICCAA 00697, 16 specs (C&S) (paratypes); CICCAA 00698, 6 specs, 1 spec. (C&S) (paratypes); CICCAA 00750, 9 specs (paratypes); CICCAA 01654, 1 spec. (paratypes); CICCAA 03385, [donated from CPUFMA 171664], 15 specs (paratypes); UFRJ 11553, 6 specs (paratypes), stream at the Anapurus municipality, Munim River, Maranhão state, Brazil. CICCAA 00089, 1 spec. (C&S) (paratypes); CICCAA 00881, 1 spec. (paratype); CICCAA 01563, 1 spec. (paratype); stream at Mata de Itamacaoca, Chapadinha municipality, Munim River, Maranhão state, Brazil. CICCAA 01382, 5 specs (paratypes); CICCAA 02008, 12 (C&S) specs (paratype), stream at Mata Fome, Barreirinhas municipality, Preguiças River, Maranhão state, Brazil. – ***H. pyrrhonotus*:** MZUSP 45714, 1 spec. (holotype), Ereré River, Brazil. – ***H. rosaceus*:** FMNH 52791, 1 spec. (holotype), Gluck Island, Essequibo River, Guyana. – ***H. wernerii*:** MZUSP 42365, 1 spec. (holotype), Santa Maria do Pará and São Miguel do Guamá municipality, Guamá River, Pará state, Brazil. CICCAA 00751, 1 spec., Paragominas municipality, Candiru River, Pará state, Brazil. – ***H. socolofi*:** MZUSP 13181, 1 spec. (holotype), Barcelos municipality, Negro River, Amazonas state, Brazil.

Appendix 2. List of nucleotide substitutions (synapomorphies and autapomorphies) from each lineage (species) and some crucial points of the cladogram of the Fig. 7B.

A (*Hypheessobrycon copelandi* clade) – COI 90 (C→A), COI 126 (A→G), COI 138 (C→T), COI 189 (C→T), COI 192 (T→A), COI 237 (C→T), COI 264 (T→C), COI 282 (C→T), COI 285 (C→A), COI 312 (T→C), COI 384 (C→T), COI 402 (A→G), COI 429 (A→G), COI 435 (A→G), COI 486 (T→C), COI 522 (A→G), COI 525 (C→T), COI 547 (C→T), COI 582 (T→C), COI 621 (T→C), COI 624 (A→G), COI 678 (T→C), COI 684 (A→C), COI 690 (T→C), COI 696 (A→G). **B** (all the species except *H. aff. copelandi*) – COI 162 (C→T), COI 270 (A→C), COI 276 (G→A), COI 363 (G→A), COI 681 (C→T). **C** (*H. aff. copelandi*) – COI 93 (G→A), COI 114 (G→A), COI 132 (T→C), COI 228 (A→G), COI 244 (C→T), COI 246 (G→A), COI 330 (C→T), COI 336 (C→A), COI 414 (T→C), COI 591 (A→G), COI 672 (T→C). **D** (*H. geryi* sp. nov.) – COI 225 (T→C), COI 228 (A→C), COI 321 (G→A), COI 522 (G→A), COI 534 (G→A), COI 543 (A→G), COI 589 (C→T), COI 615 (G→A). **E** (*H. frickei* sp. nov. + *H. copelandi*) – COI 231 (T→C), COI 315 (A→G), COI 345 (A→C), COI 375 (G→A), COI 402 (G→A), COI 405 (T→C), COI 528 (A→G), COI 558 (A→G), COI 609 (A→G). **F** (*H. frickei* sp. nov.) – COI 126 (G→A), COI 141 (G→C), COI 291 (A→G), COI 300 (A→G), COI 345 (C→G), COI 366 (C→T), COI 435 (G→A), COI 510 (T→C), COI 633 (T→C), COI 657 (C→T), COI 672 (T→C). **G** (*H. copelandi*) – COI 84 (A→G), COI 246 (G→A), COI 282 (T→C), COI 321 (G→T), COI 339 (A→G), COI 375 (A→C), COI 417 (A→G), COI 429 (G→A), COI 450 (T→C), COI 504 (T→C), COI 663 (C→T).